

# Journal of Materials Chemistry A

Accepted Manuscript



This is an *Accepted Manuscript*, which has been through the Royal Society of Chemistry peer review process and has been accepted for publication.

*Accepted Manuscripts* are published online shortly after acceptance, before technical editing, formatting and proof reading. Using this free service, authors can make their results available to the community, in citable form, before we publish the edited article. We will replace this *Accepted Manuscript* with the edited and formatted *Advance Article* as soon as it is available.

You can find more information about *Accepted Manuscripts* in the [Information for Authors](#).

Please note that technical editing may introduce minor changes to the text and/or graphics, which may alter content. The journal's standard [Terms & Conditions](#) and the [Ethical guidelines](#) still apply. In no event shall the Royal Society of Chemistry be held responsible for any errors or omissions in this *Accepted Manuscript* or any consequences arising from the use of any information it contains.

Cite this: DOI: 10.1039/c0xx00000x

www.rsc.org/xxxxxx

ARTICLE TYPE

# Biomimetic Superoleophobic Surfaces: Focusing on Their Fabrications and Applications

Ting Jiang<sup>a, b</sup>, Zhiguang Guo<sup>a, b\*</sup> and Weimin Liu<sup>b</sup>*Received (in XXX, XXX) XthXXXXXXXXXX 20XX, Accepted Xth XXXXXXXXXXXX 20XX*

DOI: 10.1039/b000000x

Superoleophobic surfaces have drawn wide attention because of their special wetting behaviour. By adjusting surface chemical composition and surface structure, different kinds of superoleophobic surfaces (in air, under water and others) can be obtained. In this account, recent progress of superoleophobic surfaces in fabrications and applications are mainly focused. The methods to fabricate superoleophobic surfaces are various and generally divided into two ways. One is top-down methods including etching, lithography, anodization and laser processing. And the other is bottom-up methods containing electrodeposition, hydrothermal method, sol-gel process and electro-spinning. But each has its own merits and demerits. Hence, choosing proper methods in different conditions are quite important. These superoleophobic surfaces can be applied in many areas, such as self-cleaning, anti-corrosion, oil transportation, anti-bio-adhesion, device, oil capture, anti-smudge, chemical shielding, micro-droplet manipulation and oil-water separation. In fact, however, few have been put into practice. The development of superoleophobic surfaces still stays in experimental stage. Current and further challenges for superoleophobic surfaces are proposed. Beyond that, some creatures with typical structure are also referred, for instance, lotus leaf, butterfly wing, rice leaf, desert beetle, rose petal, mosquito eyes, springtail, fish scale, shark skin, snail shell, the lower surface of the lotus leaf and clam's shell.

## 1. Introduction

During the past decades, increasing interests have been directed to the bio-inspired non-wetting surfaces.<sup>1-4</sup> It is well known that a surface with a water contact angle (WCA) larger than 150° and a low sliding angle (SA) is defined as superhydrophobic surface.<sup>5</sup> The same principle is also used for oil repellent surfaces.<sup>6</sup> That is so-called superoleophobic surface. The referred "oil" means organic liquid with low surface tension ( $\gamma < 72.1$  mN/m). Compared with simple superhydrophobic surfaces, the common superoleophobic surfaces in air are both repellent to water and oil because the surface free energy of oil is much smaller than that of water. From this perspective, they are also known as superamphiphobic surfaces.<sup>7</sup> Furthermore, surfaces repellent to both low and high surface tension liquids (oils) are superomniphobic surfaces.<sup>8,9</sup> Underwater superoleophobic surface, just as its name implies, exhibits superoleophobic property in water.<sup>10</sup> It is formed because of water trapping into the groove of rough structure. Meanwhile, other special superoleophobic surfaces were also developed.<sup>11-13</sup>

The history of special wetting surface can be traced back more than a century, when Ollivier et al. achieved a surface with  $\theta_{CA}$  close to 180° via coating a substrate with soot.<sup>14</sup> Thereafter, Onda et al. firstly demonstrated biomimetic superhydrophobic surfaces

in 1996.<sup>15</sup> The next year, Barthlott and Neinhuis<sup>16,17</sup> explained the principle of famous "lotus effect" in nature, and Jiang et al.<sup>18</sup> fabricated superhydrophobic surfaces by mimicking lotus leaf. In 2007, Tuteja et al. introduced the local surface curvature as the third parameter and designed the first superoleophobic surface.<sup>6</sup> In 2009, Liu et al. found that fish can keep their body clean even in polluted water and fabricated underwater superoleophobic surface by mimicking fish scale.<sup>10</sup> It is clear that the combination of low surface energy materials and suitable surface roughness is vital for the fabrication of superoleophobic surfaces. Hence, various superoleophobic surfaces are prepared constantly.<sup>19-22</sup> With the development of superoleophobic surfaces, researchers are not content with simple fabrication. Inspired from nature, superoleophobic surfaces are used for a wide range of applications, such as self-cleaning, anti-corrosion, anti-bioadhesion, oil-transportation, oil-water separation, devices and so on.<sup>23-27</sup> Meanwhile, there are still some challenges for us in biomimeticing the superoleophobic surfaces, especially in looking for more smart and convenient fabrications and their corresponding applications in industry.

To this end, it is necessary to sort out the progress of about this field in recent years, especially in the last three years, and we present an overview to make a summary about it. In the second part of the review, the creatures with special wettabilities in nature are introduced. In the third part, some fabrications are simply referred. In the fourth part, the applications of superoleophobic surfaces are focused. Finally, we make a simple

conclusion and a brief outlook on application of the superoleophobic surface, proposing their challenges and the potential solutions in the next.

## 2. Creatures in nature with special wetting surface

After billions of years of evolution, living creatures all possess unique structures in order to adapt to the environment. Lotus leaf is one of the most classic examples of special wettabilities.<sup>28,29</sup> It was discovered that lotus leaves can remain their surface clean due to the micro-andnano-structure and hydrophobic wax-like materials on their surfaces(Fig. 1a).<sup>28</sup> The butterfly wings show iridescent colours as well as superhydrophobicity by reason of multiscale structures(Fig. 1b).<sup>30,31</sup> Water droplets can roll more easily paralleling to the longitudinal direction rather than perpendicular direction on the surface of rice leaf owing to the hierarchical papillae ranged in a one dimensional order and the nanoscale waxes over the surface(Fig. 1c).<sup>32,33</sup> Namib Desert beetles collect water from fog-laden wind by right of alternative hydrophobic and hydrophilic patches on their backs(Fig. 1d).<sup>34,35</sup> Hierarchical micropapillae and nanofolds provide sufficient roughness for superhydrophobicity and high adhesion force with water on the rose petals(Fig. 1e).<sup>36</sup> Mosquito eyes have superhydrophobic antifogging property by virtue of hexagonal and non-close packed nipple at the nanoscale(Fig. 1f).<sup>37</sup> Surprisingly, there are many creatures with superoleophobic surface in nature in different surroundings.

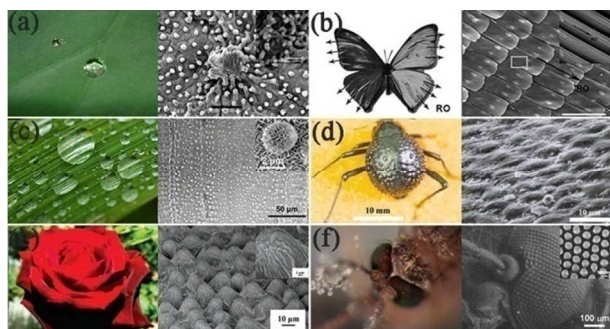


**Fig.1** The optical photos and their corresponding SEM images of creatures with special wettabilities in nature. (a) Lotus leaf and SEM images of a lotus leaf covered with micron-sized papillae and cilium-like micro-nano structure (scale bars: 50 $\mu$ m, 1 $\mu$ m).<sup>28</sup> (Copyright from Elsevier 2007) (b) Butterfly wing and SEM images of its wing covered with directional multiscale structure (scale bars: 100 $\mu$ m, 100 nm).<sup>30</sup> (c) Rice leaf and the SEM images of a rice leaf covered with oriented micro-nano structure (scale bars: 10 $\mu$ m, 2 $\mu$ m).<sup>32</sup> (Copyright from Wiley 2013) (d) Desert beetle and the SEM image of its bumpy surfaces with alternative hydrophobic and hydrophilic regions (scale bar: 10 $\mu$ m).<sup>34</sup> (Copyright from Nature 2001) (e) Rose petal and the SEM images of its surface with hierarchical micropapillae and nanofolds structure (scale bars: 10 $\mu$ m, 1 $\mu$ m).<sup>36</sup> (Copyright from ACS 2008) (f) Mosquito eyes and the the SEM images of its surfaces with nanoscale hexagonal and non-closed nipple (scale bars: 100 $\mu$ m, 100nm).<sup>37</sup>. (Copyright from Wiley 2007).

### 2.1 Springtail

Springtail, an arthropod living in shady and damp places, can

adapt to the environment by its robust and anti-adhesive skin pattern. The hexagonal comb pattern on springtail's skin is formed by small primary granules connected by ridges (Fig. 2a).<sup>38,39</sup> Moreover, papillous secondary granules also exist on the surface. The negative overhang pattern makes the skin of springtail superamphiphobic by resisting various organic liquid at evaluated pressure. When immersed in water, polar organic liquids or non-polar liquids with surface tension over 25 mJ/m<sup>2</sup>, the springtail is able to form a shiny air cushion (plastron) to prevent from wetting. In addition, the surface also shows superior resistance to microorganism.

### 2.2 Fish scale

In nature, fishes can prevent oil contamination in water, presenting excellent self-cleaning and anti-fouling.<sup>10</sup> Fish scales consist of calcium phosphate (Ca<sub>3</sub>(PO<sub>4</sub>)<sub>2</sub>), protein, and a thin layer of mucus, which makes their surfaces hydrophilic. Moreover, SEM images showed that there are oriented micropapillae covered with nanostructure on the fish scales (Fig. 2b). The existence of the hierarchical structure makes fish scales surfaces rough. The combination of hydrophilic materials and roughness leads to the surfaces more hydrophilic in air. When immersed in water, the water takes the place of the air and traps in the rough structure of fish scales surfaces, forming an oil-water-solid interface. The new composite interface exhibits superoleophobicity. The phenomena can be explained by Cassie's theory<sup>40</sup>, which refers that the air is trapped in micro/nano structured surfaces for hydrophobic surfaces in air, similar to underwater superoleophobic surfaces. The generated oil-water-solid interface prevents oil from contacting with the solid substrates, making the oleophobicity increase. When roughness continues to increase, the surface may become superoleophobic.

### 2.3 Shark skin

Shark skin is especially attractive because of its low fluid drag and oleophobicity with low adhesion.<sup>41-44</sup> The shark skin is covered by many small single tooth-like scales called dermal denticles, which include riblets oriented parallel to the local direction of water flow (Fig. 2c). When the shark swims quickly, the riblets are beneficial to lift and pin the vortices formed in the viscous sublayer, making the drag reduce. It is believed that the riblets on shark skin can increase water flow rate at the solid-liquid interface. Furthermore, the surrounding water makes for protection from marine fouling and organisms. Hence, the special structure of shark skin not only make shark swim rapidly and efficiently in water but also help prevent from marine fouling and bio-adhesion, exhibiting a self-cleaning property.

### 2.4 Snail shell

Snail is common on rainy days, the shell of which exhibits self-cleaning property.<sup>45</sup> The snail shell is composed of a composite of aragonite and protein, and covered with a protein layer. In addition, rough structure with line grooves is on the top surface of snail shell. The rough structure of snail shell shows high regularity (Fig. 2d). Hence, the hydrophilic material and rough

structure lead to the superoleophobicity in water. Studies show that the superoleophobic property under water makes the snail shell clean. Thus, the wet surface of the snail shell is hard to be contaminated.

### 2.5 The lower surface of lotus leaf

It is known that the upper surface of the lotus leaf is superhydrophobic. But little noticed that the lower surface of the lotus leaf is different from its upper surface. Cheng et al. discovered that the lower surface of the lotus leaf is superoleophobic in water and also have the ability of self-clean.<sup>46</sup> The rough structure of its lower side consists of many tabular and slightly convex papillae (Fig. 2e). Every individual papilla is covered with nanogroove structures. In addition, certain hydrophilic material like ferns may exist on the surface.<sup>47</sup> The combination of hydrophilic compound and the hierarchical micro/nano structure makes the lower surface hydrophilic in air and superoleophobic in water.

### 2.6 Clam's shell

The shell of clam, both outside and internal surface, can always remain clean in nature. Take internal surface for example, it can be divided into two regions: the glossy edge region (region 1) and coarse inside region (region 2) (Fig. 2f).<sup>48</sup> Region 1 was contaminated with crude oil while region 2 remained clean after oleophobic test. There is little difference in chemical composition of the two regions. But the distinction in surface structure is of great significance. Region 1 is relatively smooth with micrometer-scale leaf-like slices. At region 2, micrometer-scale irregular chunks heap with many nanometer-scaled blocks, showing a rather rough morphology. Generally, hydrophilic surface in air may lead to oleophobicity in water.<sup>10</sup> It is the hydrophilic  $\text{CaCO}_3$  that make the shell of clam surface underwater oleophobic. Besides, the hierarchical micro/nano structure in region 2 lead to more water-wetting, giving rise to superoleophobic and low adhesion. Which is for sure, by integrating superior mechanical performance inspired by such shell with remarkable superoleophobicity mentioned above, a wider range of applications can be realized and progressed.<sup>49-53</sup>

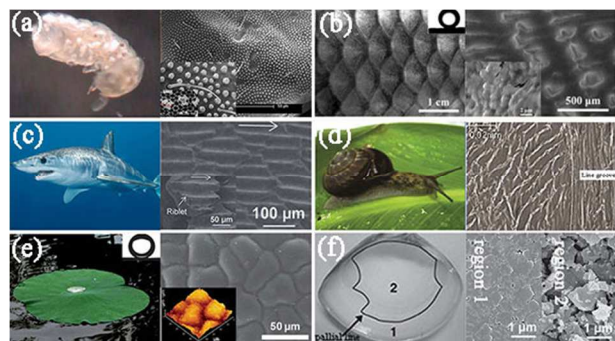


**Fig. 2** Photographs of creatures with superoleophobic surface in nature: (a) (left) Orthonychiurus stachianus immersed in ethanol resist wetting through the formation of a shiny air cushion, (right) the SEM images of Orthonychiurus stachianus at different magnification<sup>38</sup> (b) (left) photograph of fish scale and its oil

contact angle (OCA) in water, with a OCA of  $156.4 \pm 3.0^\circ$ , (right) the SEM images of fish at different magnification<sup>10</sup> (c) (left) the optical photo of mako shark, (right) the SEM image of shark skin at different magnification<sup>44</sup> (d) (left) the optical photo of snail shell, (right) the SEM image of snail shell<sup>45</sup> (e) (left) the photo of the lotus leaf and its OCA, with a OCA of  $155.0 \pm 1.5^\circ$ , (right) the ESEM and AFM (insert) image of the lower surface of the lotus leaf<sup>46</sup> (f) (left) the photo of clam's shell, (right) the SEM image of region 1 and region 2, respectively<sup>48</sup>. (Copyright from Wiley 2012)

Except for the creatures mentioned above, others also have special wettability.<sup>54-56</sup> These phenomena are caused by their surface geometrical structure and surface free energy. Inspired by these, many similar surfaces can be designed.<sup>57-61</sup>

## 3. Fabrications of superoleophobic surfaces

Inspired from nature, a lot of superoleophobic surfaces have been designed via various methods. To the best of our knowledge, the appropriate surface roughness and surface chemistry are both crucial factors to the fabrication of superhydrophobic surfaces. And the demands are even stricter for superoleophobic surfaces in air. Suitable low surface energy materials, like fluorinated compound and thiol, are important to superoleophobic surfaces. For surface roughness, simple micro/nano dual scale structure is not enough. A new idea of re-entrant geometry structure, such as T-shape<sup>62</sup>, overhanging<sup>63,64</sup> and mushroom-like<sup>65</sup>, is introduced into the construction of superoleophobic surfaces.<sup>20,66</sup> On the contrary, hydrophilic materials (eg.  $\text{CaCO}_3$  and  $\text{Ca}_3(\text{PO}_4)_2$ ) and hierarchical micro/nano structure are vital for underwater superoleophobic surfaces. As it mentioned above, water molecules can be easily trapped into the groove of micro/nano structure because of its hydrophilicity, thus forming a composite water-solid interface. Hence, the composite interface lead to oleophobic and low-adhesive surfaces in water. According to Wenzel's model<sup>67</sup>, the hydrophilic surfaces will be more hydrophilic and the hydrophobic surface will be more hydrophobic with the increase of the roughness. Therefore, more water will be trapped in the rough structure of hydrophilic surfaces, and finally make the surface superoleophic.

The fabrication methods are quite rich and they are often divided into two basic approaches. One is top-down method, and the other is bottom-up method. The former is beneficial to achieve a surface topography with highly controlled, and the latter usually leads to a randomly structure.<sup>68</sup> However, the former is more difficult to put into effect.

### 3.1 Top-down methods

**3.1.1 Etching.** Etching is a facile and low-cost process to produce rough structure and widely used for the fabrication of superoleophobic surfaces. It can be separated into wet etching and dry etching based on whether the solutions are in use. It is prone to product and repeat with simple devices for wet etching. But the surface topography is difficult to be well controlled, especially for small-sized materials. Compared with wet etching, dry etching is easy to be controlled and has no waste liquors. However, the required equipment is more complex and more expensive. In addition, the surfaces created by both wet etch and

dry etch are fragile because of the removal of material from original surfaces.

Using Al as the substrate, Ji et al. have prepared lotus-like hierarchical structure with HCl containing isopropyl alcohol (IPA).<sup>69</sup> Surface fluorination is needed for superoleophobicity. Copper substrate is also used to fabricate superoleophobic surfaces by etching. Zhao et al. prepared microflowers and nanorod arrays hierarchical structure on copper substrates by immersing it into a mixed solution of NaOH and ammonium persulphate ((NH<sub>4</sub>)<sub>2</sub>S<sub>2</sub>O<sub>8</sub>).<sup>70</sup> Combining with acid etching and base etching, Ou et al. prepared the micro/nano hierarchical structure of superoleophobic surfaces on copper substrate.<sup>71</sup> They successively immersed the pre-treated copper substrates in an aqueous solution of HNO<sub>3</sub> and cetyltrimethyl ammonium bromide as well as an aqueous solution of NaOH and (NH<sub>4</sub>)<sub>2</sub>S<sub>2</sub>O<sub>8</sub>. Song et al. prepared a superoleophobic surface with a peanut oil CA of 160.0±2° via electrochemical etching and then immersing in [Ag(NH<sub>3</sub>)<sub>2</sub>]<sup>+</sup> solution. Finally, perfluorooctanoic acid (PFOA) was used to reduce the surface energy of the prepared micro/nano structure.<sup>72</sup> Random or ordered hierarchical micro-nano texturing was obtained by Ellinas et al. using plasma texturing on polymeric surface.<sup>73</sup>

**3.1.2 Lithography.** In particular, the technique can allow the precise control of the structure on the surface of workpiece. In other words, surfaces patterned with different shapes and different sizes can be prepared by this method.<sup>74-76</sup> The advantage for lithography is that the template is easy to be fabricated and used for many times, leading to a lower cost. Furthermore, the obtained structures and morphology of surfaces are various. It needs a long molding cycle and it is liable to produce defects in the process of lithography.

Cai et al. fabricated artificial anisotropic superoleophobic surfaces via soft lithography and following oxygen-plasma treatment by mimicking the oriented hood-like structure of filefish on polydimethylsiloxane (PDMS) layers (Fig. 3a).<sup>58</sup> The OCA of the artificial PDMS filefish skin is 143±2.1° in water, exhibiting an anisotropic oleophobicity. This method can be used for simple mass production of cheap material with high surface energy and was proved on commercial cloth corduroy. By the combination of ultraviolet nanoimprint lithography (UV NIL) and hydrothermal synthesis, Jo et al. fabricated superamphiphobic surfaces based on ZnO nano-in-micro hierarchical structure (Fig. 3b).<sup>77</sup> They firstly prepared a ZnO nano-particles dispersion resin and then patterned a circular cone shaped micro-pattern with the as-prepared resin by UV NIL. Subsequently, ZnO nanorods were grown on the surface of the micro-pattern by low temperature hydrothermal synthesis. The values of CA for diiodomethane on the obtained surfaces were more than 155° with low contact angle hysteresis (CAH). Therefore, the simple process can also be used to fabricate surfaces on a large scale on various substrates including Si wafer, glass, and PET film. Other structures were also obtained via the similar methods. Lee et al. designed superamphiphobic surface with nanoscale re-entrant curvature (Fig. 3c) via nanotransferred molding and isotropic etching.<sup>64</sup> Choi et al. prepared superamphiphobic surfaces with overhang structures (Fig. 3d) via reverse nanoimprint lithography.<sup>78</sup> The CAs on simple overhang surface for water, diiodomethane, and hexadecane are 164°, 151°, and 114°, respectively.

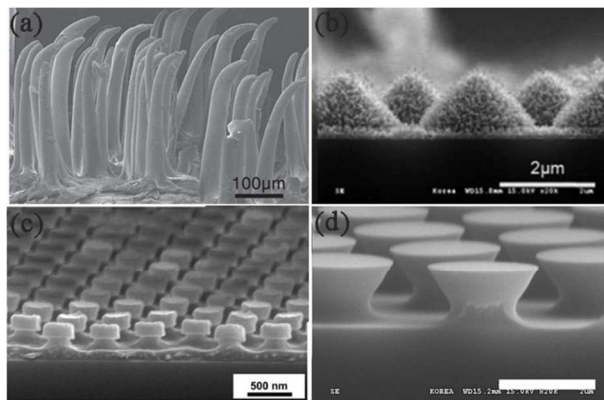


**Fig. 3** Various structures prepared by lithography. (a) The hood-like spine of artificial skin.<sup>58</sup> (b) Nano-in-micro hierarchical structure.<sup>77</sup> (c) Nanoscale re-entrant curvature.<sup>64</sup> (Copyright from ACS 2013) (d) Simple overhanging structure.<sup>78</sup> (Copyright from ACS 2013)

**3.1.3 Anodization.** Anodization is a kind of metal surface treatment that the surfaces of metal and its alloy form oxide film through the impressed anodic current in the electrolyte solution. It is often served as a material protection technology.

TiO<sub>2</sub> is a popular semiconductor metal oxide because of its excellent photocatalytic oxidation activity and photoinduced superhydrophilicity.<sup>79,80</sup> The TiO<sub>2</sub> nanotube arrays are easily and tightly formed on the entire surface of the Ti substrate through anodization.<sup>81</sup> Inspired by this, Barthwal et al. fabricated a superamphiphobic Ti surface via anodization.<sup>82</sup> First, they constructed a microstructured Ti surface by electrochemical etching in a 0.1 M NaCl solution. Then, the microtextured Ti surface was further anodized to obtain TiO<sub>2</sub> nanotube arrays. Finally, a solution of 1H,1H,2H,2H-perfluorooctyltrichlorosilane and n-hexane was used to reduce the free energy of the micro/nano structure surface. The anodized surface maintained good superamphiphobic stability with long-term storage. Furthermore, the technique can be used for other substrates of large areas. Nishimoto et al. also prepared superoleophobic surfaces on Ti substrates by anodization.<sup>83</sup> First, either Ti plate or Ti mesh was anodized in 0.3M NH<sub>4</sub>F solution containing 3vol% of deionized water to obtain TiO<sub>2</sub> nanotube arrays. After rinsing, the sample was calcined at 500 °C for 1h. Thus, the underwater superoleophobicity was realized. Al is another common substrate to design superoleophobic surface in anodization. Barthwal et al. designed mechanically robust superamphiphobic surfaces with down-directed nano structure.<sup>84</sup> The referred methodology contains: (1) form the micro-structure by etching in acidic solution (2) form nanopores by anodizing in H<sub>2</sub>SO<sub>4</sub> solution, (3) fluorination. The fabrication technique is simple and time-saving, and can be used on any other substrates on a large area. In addition, the resultant down-directed structure made from nanopores makes the superamphiphobic surface more robust and more durable.

The method is simple, low-cost, and fast. However, the surfaces prepared by anodization are often nonuniform and have many defects. In addition, the residual solution may pollute the environment.

**3.1.4 Laser processing.** Laser processing has emerged as a new method to construct special surface topography. It has many advantages over traditional methods. It is a one-step method

without any mask and the environment needed is not harsh. Further, the structures of surfaces can be controlled by adjusting parameters, such as scanning speed, pulse number and laser fluence. Particularly, laser can realize complex multiple-wettability integration without fluorination.

Yong et al. prepared underwater superoleophobic surfaces via femtosecond laser micromachining on a flat Si surface through a line-by-line and serial scanning process.<sup>85</sup> The laser energy was 20 mW, and the scanning speed was 2 mm s<sup>-1</sup>. There were many spike-like structures on the surface (Fig. 4a), and each was covered with many nano-sized protrusions. The micro/nano structure dispersed uniformly on the surface (Fig. 4b). The WCA of the laser-induced surface is nearly 4° (Fig. 4c) and the OCA of that is 159.4° (Fig. 4d) in water, exhibiting superhydrophilic in air and superoleophobic in water. The 6 μL and 8 μL oil (1,2-dichloroethane) droplets were used to test ultra-low oil adhesion on the as-prepared surface, respectively (Fig. 4e). During the contacting and leaving process, no residual oil was left on the surface. And the oil droplet can easily roll on the tilted surface of 0.5°. The method is simple and can precisely control processing location.

However, the development of the laser processing is still in its infancy and the underlying mechanism is unclear. Besides, processing speed and throughput are expected to be improved.

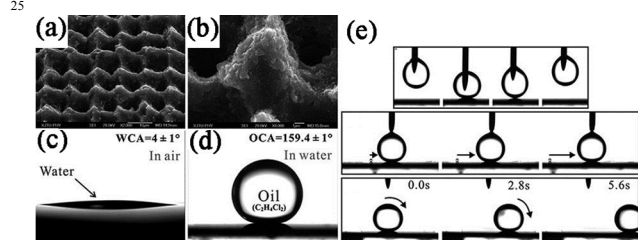


**Fig. 4** The SEM images of the laser-induced surface and its wetting behaviors. 45° tilted view SEM image with the magnification of (a) 2000 and (b) 8000. (c) Shape of a water droplet on the rough surface in air, showing superhydrophilicity. (d) Shape of oil (1,2-dichloroethane) droplet on the rough surface in water, showing underwater superoleophobicity. (e) Oil-adhesion of the femtosecond laser structured surface.<sup>85</sup>

### 3.2 Bottom-up methods

**3.2.1 Electrodeposition.** Contrary to electrochemical etching, electrodeposition is aimed at covering the substrate with a layer of metal. The surface morphology can be controlled by changing monomer structures and the electrochemical parameters. The only condition for electrodeposition is that the surfaces are conductive and difficult to be oxidized.

Fluoropolymers, especially for long chains, are often used for the fabrication of superoleophobic surfaces.<sup>86</sup> But, the toxicity greatly limits their applications. Combining with short fluorinated chains and electrodeposition, a series of superoleophobic surfaces were designed by Darmanin et al.<sup>66,87-89</sup> They designed superoleophobic surfaces through electrodeposition of original fluorinated 3,4-ethylenedioxythiophene (EDOT) derivatives containing an amide connector, which was synthesized from 3,4-dimethoxythiophene via a three-step procedure.<sup>66</sup> They found that the superoleophobic properties ( $\theta_{\text{sunfloweroil}} = 150.0^\circ$  and  $\theta_{\text{hexadecane}} = 132.1^\circ$ ) are only obtained with F-butyl tails. They also designed superoleophobic ( $\theta_{\text{sunfloweroil}} = 150.0^\circ$  and  $\theta_{\text{hexadecane}} = 136^\circ$ )

meshes with high adhesion via electrodeposition of conductive polymer including C<sub>4</sub>F<sub>9</sub> chains on stainless steel surfaces.<sup>88</sup> The micro/nano structures were created by applying high deposition charge ( $Q_s = 225 \text{ mC} \cdot \text{cm}^{-2}$ ). Polymers with C<sub>4</sub>F<sub>9</sub> chains provide new strategies to design superoleophobic surfaces with low bioaccumulative potential. In addition, they designed superoleophobic surfaces via electrodeposition bonding with fluorinated monomer and hydrocarbon monomer, which both have the same 3,4-ethylenedioxythiophene (EDOT) core.<sup>90</sup> Results showed that the surfaces exhibited good wettability for water, sunflower oil, hexadecane, dodecane and octane when EDOT-F<sub>8</sub> molar proportion above 75%.

**3.2.2 Hydrothermal method.** Hydrothermal method is another useful technique to create roughness.<sup>91</sup> The products are high purity uniformly disperse. In addition, the morphology of the product is beautiful and well controlled. The principle of the hydrothermal method is to dissolve substances making use of high temperature and high pressure. Hence, the requirement for devices is rather high and it is both difficult and dangerous to operate, which hinders the large-scale production of superoleophobic surfaces and makes it unsuitable for practical applications.

Wang et al. prepared an underwater superoleophobic coating based on hierarchical rutile TiO<sub>2</sub> flowers through a simple one-step hydrothermal method.<sup>92</sup> First, 1 g of Zn (CH<sub>3</sub>COO)<sub>2</sub>·2H<sub>2</sub>O and 20 ml of concentrated hydrochloric acid (36-38wt%) were dissolved in 30 ml of deionized water successively and the mixture was stirred for 5 min. Then, 1 ml of titanium isopropoxide was added. After stirring for another 5 min, ultrasonically cleaned fluorine-doped tin oxide (FTO) substrates were placed into the Teflon-lined stainless steel autoclave. The hydrothermal reaction was occurred at 140 °C for 9 h. The flower-like structure made up of many petals on the obtained surface (Fig. 5a) and each petal consisted of many ultrathin nanoneedles (Fig. 5b). Beyond that, these obtained coatings showed superamphiphilicity in air and superoleophobicity in water with an OCA of 155° (Fig. 5c,d and e). Zeng et al. also fabricated an underwater superoleophobic silicalite-1 (MFI) zeolite-coated film.<sup>93</sup> The MFI crystal seeds were firstly synthesized by hydrothermal method using Tetrapropylammonium bromide (TPABr) and n-butylamine. Then, the superoleophobic MFI zeolite-coated films were obtained by secondary growth. The as-prepared film exhibited good durability and can be used in harsh conditions.

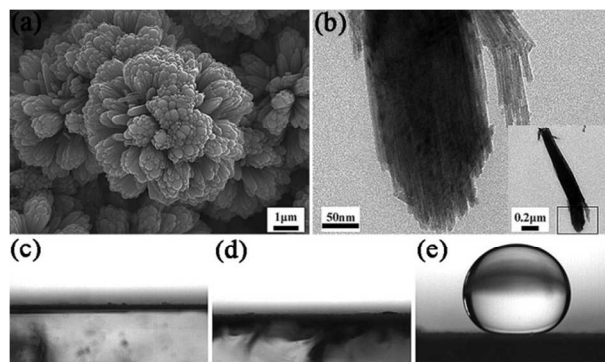


**Fig. 5** (A) The FE-SEM image of the hierarchical rutile TiO<sub>2</sub> flowers. (B) The TEM image of the single petal. (C) Water and (D) oil droplet on the surface, indicating a superamphiphilicity of the coatings. (E) An oil droplet on TiO<sub>2</sub> coatings in water,

exhibiting a superoleophobic property.<sup>92</sup> (Copyright from AIP 2014)

**3.2.3 Sol-gel process.** Sol-gel approach is one of the wet chemical methods and usually carries out in mild conditions. To be specific, it can be performed at low temperature. In addition, the approach is simple and low-cost. However, the process is very slow and may need several hours and even several days.

Hayase et al. have fabricated the first superamphiphobic monolith by using vinyltrimethoxysilane (VTMS)-vinylmethyldimethoxysilane (VMDMS) co-precursor system.<sup>94</sup> The co-precursor system was prepared as follows (Fig. 6a). First, VTMS, VMDMS, urea, surfactant n-hexadecyltrimethyl ammonium chloride (CTAC) were mixed in a dilute acetic acid solution and stirred at room temperature for 60 min. Then, the prepared sol was transferred to an oven for gelation and aging at 80 °C for several hours under basic conditions. Next, the sample was washed with alcohol and evaporative drying under ambient conditions. The obtained gel (MG1) merely showed superhydrophobic property. In order to achieve superoleophobicity, MG1 was immersed in a 2-propanol solution containing 1H,1H,2H,2H-perfluorodecanethiol (10 v/v%) with a radical initiator N,N'-azobisisobutyronitrile (AIBN)(Fig. 6b). After the treatment, the obtained gel (MG2) acquired superoleophobicity and the contact angle of n-hexadecane is 151°. And no changes were found on the SEM images (Fig. 6c and d). Li et al. prepared a superamphiphobic surface by a facile method.<sup>95</sup> First, they fabricated SiO<sub>2</sub>-CNTs hybrid material through sol-gel method. 1 g hydroxyl MWCNTs were dispersed in 100 ml ethanol. Subsequently, 5mL ammonia aqueous solution (25 wt %) and a 27.5 mL mixture of TEOS and ethanol (volume ratio 1:10) was added dropwise into the dispersion prepared above under the magnetic stirring, respectively. The mixture need to be kept stirring at room temperature for 12 h. Then, the SiO<sub>2</sub>-CNT suspension was sprayed on glass slides. Finally, the sample was fluorinated. The as-prepared coatings can be repellent to water and other organic liquids. The whole process is simple so that it can be used for mass production.

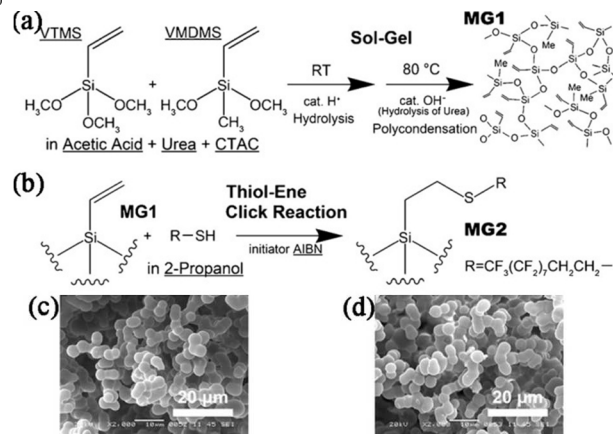


**Fig. 6** (a) One-pot synthesis for the VTMS-VMDMS marshmallow-like gel (MG1). (b) Synthetic approach for the oleophobic MG2. (c) The SEM image of MG1. (d) The SEM image of MG2. From SEM observations, no changes are found in the macroporous morphology by the reaction.<sup>94</sup> (Copyright from Wiley 2013)

**3.2.4 Electrospinning.** Electrospinning is an inexpensive, simple, scalable and universal method to produce nonwoven micro/nanofiber with high specific surface area and porosity directly and continuously.

Kota et al. have developed a simple one-step technique based on electrospinning microbeads onto textured surfaces to fabricate superoleophobic surfaces with re-entrant structure.<sup>96</sup> The prepared superoleophobic surfaces exhibited ultralow contact angle hysteresis (CAH) even for extremely low surface tension liquids (the roll angle of n-heptane was less than 2°, which was oleophilic). Ganesh et al. prepared robust superamphiphobic self-cleaning coatings on glass substrates.<sup>97</sup> The rice-shaped TiO<sub>2</sub> nanostructures were prepared by electrospinning and subsequently silanization. The WCA and OCA (ethylene glycol) were 166° and CA=152.6°, respectively. The CAH for the droplet of water and hexadecane were 2° and 12°, respectively. In addition, the coatings showed excellent mechanical and thermal stability with high adherence to glass substrates. Ahmed et al. have prepared underwater superoleophobic composite membranes via electrospun polyvinylidene fluoride-co-hexafluoropropylene (PVDF-HFP) nanofibers and then modified with cellulose.<sup>98</sup> The membranes showed excellent mechanical properties, wettability, pore size and porosity.

Nevertheless, it is hard to obtain the nanofibers separated from each other via electrospinning and the strength of the obtained nanofibers is relatively low. In addition, the mechanical adhesion between electrospun fibers and substrates has yet to be improved.

**3.2.5 Others.** Other bottom-up methods for superoleophobic surfaces have also been reported, such as spray deposition<sup>99</sup>, dip coating<sup>100</sup>, self-assembly<sup>101</sup>, vapor deposition<sup>102</sup> and template method<sup>103</sup>.

Though these methods can be applied to fabricate superoleophobic surfaces, few can be used in industrial production because of their expensive cost, and limited production conditions. In addition, the stability of the obtained surfaces is also needed to be improved. Hence, many superoleophobic surfaces with stable mechanical behavior were designed.<sup>84,104</sup>

## 4. Applications

### 4.1 Superoleophobic-superhydrophobic surfaces in air

Because of the excellent properties of the superoleophobic surfaces, much attention has been paid to their applications. And the scientists have made great progress in some areas. The detailed introductions are as follows.

**4.1.1 Self-cleaning.** To the best of our knowledge, lotus leaf has extraordinary self-clean ability.<sup>29</sup> The dirt can be easily taken away as the sliding of water droplet on the surface, thus making it clean. Inspired from nature, the scientists have successfully fabricated many materials with self-clean ability.<sup>105,106</sup> And many of them have been put into practice, like windshield, exterior wall. However, when meeting with oil, the structure is damaged, causing superhydrophobicity to decrease, even disappear. Therefore, the idea of constructing superoleophobic surfaces is very important. Due to the high contact angle and low sliding angle for water and oil, superoleophobic surfaces have good self-cleaning ability for both water and oil. Yuan et al. reported a direct generation of linear polyethylenimine (PEI) and silica thin films.<sup>107</sup> The obtained films showed super-repelling property to various liquid, such as commercial inkjet (IJ) ink, soy source, and

milk. Furthermore, the complex liquid contaminated surfaces can be easily and completely cleaned by simply water drop flow. Importantly, the surface still remained self-clean ability after ultrasonication treatment in ethanol for 7 h. Das et al. have developed conductive polymer carbon nanofiber/fluoropolymer composite films.<sup>108</sup> The static water and oil contact angles varied with the changes of the concentration of carbon nanofiber and polymer. And some coatings with the highest contact angles for oil and water took on self-cleaning property (liquid roll-angle less than 10°). Zhao et al. prepared a directional self-cleaning superoleophobic surface on silicon wafer by photolithography and modified with fluorosilane.<sup>24</sup> Because of the parallel grooves on the resultant surfaces, it exhibits anisotropic self-cleaning ability. The mobility increased in the parallel direction while retarded in the vertical direction, which is similar to butterfly wings, rice leaves, duck feathers.<sup>109-111</sup> These self-cleaning surfaces can be used in buildings and coatings. This will benefit to our daily life.

**4.1.2 Oil-transportation.** In the transportation of crude oil, crude oil will easily stick to the pipeline, making severely blocking and loss. This has become a serious problem. A lot of measures have been taken, for example, solvent injection<sup>113</sup> and magnetic fields<sup>113</sup>. But, they took little effects. Inspired from the special wetting surface in nature, the scientists find a new way to solve the problem. In general, liquids are transported by other immiscible liquids as flow carriers.<sup>114</sup> However, a new idea of oil-based microreactor is proposed. Yao et al. fabricated various superoleophobic surfaces of controllable oil adhesion via perfluorothiolate reaction on Cu(OH)<sub>2</sub> nanostructure surfaces.<sup>115</sup> The application for oil droplet-based microreactor in oil transportation was also demonstrated. The oil droplet containing styrene monomer was deposited on superoleophobic surface of low adhesion and subsequently captured by metal cap. Next, the original oil droplet contacted with the oil droplet containing Br<sub>2</sub> on the superoleophobic surface of high adhesion, and then coalesced with color fading. Finally, the merged droplet was remained on the superoleophobic surface of high adhesion. Hence, this method can be used for no-loss oil transportation.

**4.1.3 Oil capture.** One of the anti-oil routines is based on oleophilic materials that are able to absorb oil. But the oil on the oleophilic surfaces is hard to remove. Hence, it is a waste of oil and oleophilic materials. According to a derived formula of Young's equation<sup>116</sup>, the amphiphobic surfaces in air might be oleophobic or oleophilic in water. Learning from this, Jin et al. designed a novel organosilane surface, which is superamphiphobic in air and superoleophilic under water via phase separation reaction.<sup>117</sup> They also tested the ability of collecting oil droplets in water (Fig. 7). Oil droplets can be captured by a 1H,1H,2H,2H-perfluorodecyltrichlorosilane (FTS)-derived glass tube in water. It is well-known that superhydrophobic/superoleophilic surfaces also can be used to gather oil droplets from water. The main difference is that the absorbed oil droplets are able to fall off from the glass tube automatically and quickly for designed surface in air. But the superhydrophobic/superoleophilic surfaces are totally wetted and polluted by oil. Moreover, the obtained superamphiphobic surface can be reused because of its special wettability.

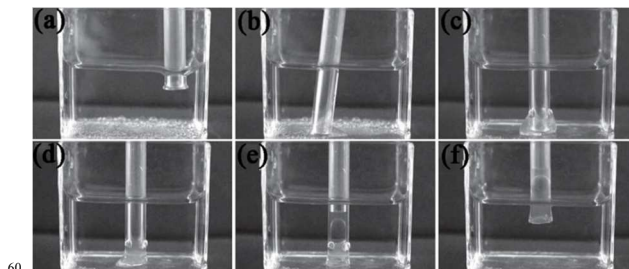


**Fig. 7** The processes of oil capture and oil collection using a FTS-derived glass tube in water. (a) A layer of oil droplets was deposited in the bottom of a water container, and the tube was approaching to the oil droplets. (b) The glass tube touched and collected the oil drops underwater. (c) As the glass tube was moved in water, oil droplets were gathered together. (d-f) The oil droplets were extracted from the water.<sup>117</sup> (Copyright from Wiley 2011)

**4.1.4 Anti-smudge.** Recently, touch screens have played an important role in our daily life, such as cell phones, music players, and tablet computers, which generates a new problem on anti-smudge of screens. The fingerprint, bacteria, and dust on those screens are inevitable, and make them dirty. At present, people are trying to find applicable ways to solve the problem. Since the main component of fingerprint is oleic acid, the oleic acid contact angle is used to evaluate the anti-fingerprint property.<sup>23</sup> If the surface is oil-repellent, it will have good anti-fingerprint ability. Essentially, it reduces the adhesion of the fingerprint on the surface. Over the years, many literatures about anti-fingerprint are reported.<sup>118,119</sup> Bhushan and Muthiah presented a novel way to characterize anti-smudge properties.<sup>120</sup> Oil-impregnated microfiber wiping cloth was used to test two artificially contaminated coatings. After the test, in dual-layered superoleophobic surface, almost all contaminant were cleaned and adhered on oil-impregnated cloth while partial contaminant were cleaned and attached in single-layered coatings. The results showed that the dual-layered superoleophobic surface had the ability to remove contaminants and thus exhibited anti-smudge. The tested superoleophobic surface was prepared through hydrophobic SiO<sub>2</sub> nanoparticles, fluorinated acrylic copolymer, and PTFE amorphous fluoropolymer by dip coating and spray coating techniques on glass substrates.<sup>121</sup> But it is not limited to glass substrates. Moreover, it doesn't need any chemical post treatment process.

**4.1.5 Corrosion resistance.** Many materials, like copper (Cu) and iron (Fe) are easily corroded after a period of time, which severely hinder their use. With the purpose of overcoming this flaw, many steps have been taken.<sup>122-124</sup> Recently, researches show that making their surfaces superoleophobic can improve corrosion resistance with effect. Yuan et al. prepared superamphiphobic surfaces on common cast iron substrates.<sup>125</sup> No rust, color and weight change were observed on the obtained superamphiphobic surfaces when they were kept in an ambient environment for 6 months. While the untreated cast iron changed a lot. Zhang et al. fabricated superoleophobic surfaces with enhanced corrosion resistance on copper sheets.<sup>26</sup> Interestingly, the surfaces can be recovered by a simply regeneration process after losing the superoleophobicity. The obtained surfaces are expected for large-scale production. Motlagh et al. prepared a durable, superamphiphobic and corrosion resistant coating on the stainless steel surface.<sup>126</sup> Results showed that the films could maintain superamphiphobic after immersing in water for 16 days, and the highest protection efficiency could reach 97.33%. In consequence of simplicity of preparation process, the coatings can be applied to a variety of substrates on a large scale. Ge et al. prepared superamphiphobic coatings on copper substrates by



spray coating (Fig. 8a).<sup>127</sup> They examined the corrosion behavior of the as-prepared superamphiphobic surface through potentiodynamic polarization tests (Fig. 8b). The results show that the as-prepared superamphiphobic surface have higher positive of  $E_{\text{corr}}$  and lower  $I_{\text{corr}}$ , indicating a good corrosion resistance.<sup>128</sup> When in Cassie state, oxygen is restricted to contact with Cu surface since air can easily trap in the valleys between the protrusions. Furthermore,  $\text{Cl}^-$  and water are also difficult to touch the surface. All of these are the factors that superamphiphobic coatings have favorable anti-corrosion ability. The mentioned methods are not confined to certain metal but for widespread materials, which makes for the mass production on various substrates and greatly extends their application.

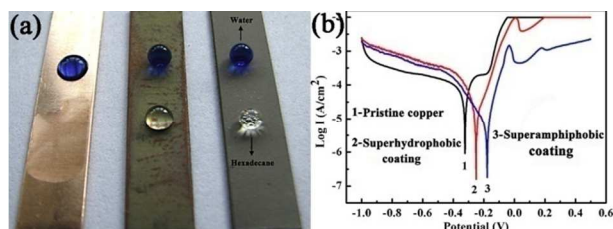


**Fig. 8** (a) The optical image of water and hexadecane droplets placed on the pristine copper surface, superhydrophobic surface, and superamphiphobic surface, respectively. (b) Potentiodynamic curves of the pristine copper surface, superhydrophobic surface, and superamphiphobic surface, indicating the excellent anti-corrosion ability of superamphiphobic surface.<sup>127</sup> (Copyright from Elsevier 2014)

**4.1.6 Chemical shielding.** Superoleophobic surfaces can protect from many chemicals in addition to water because of its excellent ability to repel various liquids. That is to say, besides anti-corrosion ability, they also show good chemical shielding. For example, Pan et al. prepared a superomniphobic surface which not only was repellent to Newtonian liquids but also to a lot of non-Newtonian liquids, showing excellent chemical resistance to different chemicals.<sup>129</sup> When immersed in concentrated hydrochloric acid (HCl) and concentrated sodium hydroxide (NaOH), the uncoated side of Al plate was damaged, while the coated side remained unchanged (Fig. 9a-f). Beyond that, some inorganic or organic liquid droplets that adversely affect PDMS, all can bounce and roll on the surface. When immersed in poly (dimethylsiloxane) (PDMS), a bright plastron was appeared, and it still stable and remained unchanged even when exposed to un-cross-linked PDMS (Fig. 9g). Hence, the surface can shield against almost all liquids effectively.

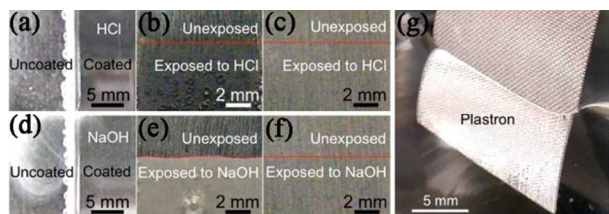


**Fig. 9** (a and d) Side view of an aluminium plate immersed in concentrated hydrochloric acid (HCl) and concentrated sodium hydroxide (NaOH), respectively. One side of the plate is uncoated, while the other side is coated with the as-prepared coating. (b and e) The uncoated aluminum surface appears rough and damaged after immersion in HCl and NaOH, respectively. (c and f) The coated aluminum surface remains unaffected after immersion in HCl and NaOH, respectively. (g) A bright plastron

layer is visible when the surface is immersed in a liquid bath of PDMS.<sup>129</sup> (Copyright from ACS 2013)

**4.1.7 Printing.** Over the years, Teflon materials, such as PTFE, have been used for printing on account of their chemical inert and thermal stability. Law et al. measured the contact angles of a series of liquids including water, hexadecane, ink and toner.<sup>130</sup> They found that the PTFE was highly hydrophobic but actually oleophilic and sticky. Hence, replaceable materials are expected for future print industry. Inspired by nature, the interaction force between print surface and imaging materials can be well controlled. After fusing, image quality defect caused by toner adhesion of the fuser surface is called offset, which is highly undesirable in printing. In order to circumvent offset during fusing, Zhao et al. designed a model superoleophobic surface on silicon wafer via photolithography and surface modification with FOTS.<sup>131</sup> Compared with superhydrophobic Si surfaces obtained from i-CVD PTFE coating, the resultant superoleophobic Si surfaces showed much lower adhesion between imaging materials and fuser surface. This will benefit for better imaging quality and less materials cost.

**4.1.8 Micro-droplet manipulation.** One limitation that hinders broader applications for digital microfluidics is surface biofouling.<sup>132,133</sup> Freire et al. designed a new strategy to transport liquid droplet containing cells and other analytes on solid substrates without any additive through a superamphiphobic surface assisted with field dewetting device for the first time.<sup>134</sup> The droplets of different volumes were merged immediately. The droplets of similar volumes, however, tended not to recombine due to the existence of repulsive force. The surface is easy to fabricate with little resources. Moreover, it can be transferred to other substrates and reused. The main problem, however, is that the Teflon solution partially or even completely washed away the soot during the coating process.

**4.1.9 Transparent superamphiphobic coatings.** Optical surfaces that can repel both water and oil have been an indispensable part in our life including solar panels, windshields, and touch screens.<sup>135</sup> Both the superoleophobicity and transparency are crucial to them. It is clear that the surface roughness is one of the vital factors to superoleophobic surfaces. But the transparency is exactly the opposite. Generally, the transmittance decreases as the increase of the roughness mainly due to light scattering.<sup>136,137</sup> So, the design of transparent superoleophobic surfaces is more complex. In recent years, many transparent, robust, superamphiphobic coatings were prepared by using different templates.<sup>103,138</sup> Using candle soot as a template, a transparent superamphiphobic coating was designed by Deng et al.<sup>103</sup> The transparency of the coatings was verified by ultraviolet-visible transmittance spectra (Fig. 10a). It can be easily seen that the transmittance of the as-prepared superamphiphobic coatings was reduced by less than 10% compared with that of pristine glass when wavelengths was above 500 nm (the thickness of coatings was 3- $\mu\text{m}$ ). This transparency was also reflected in the visibility of words under the coated glass plate (Fig. 10b). Ganesh et al. prepared another transparent superamphiphobic surface utilizing electrospun  $\text{SiO}_2$  nanofibers as a template.<sup>138</sup> The CA of the prepared surfaces for water and hexadecane were  $161^\circ$  and  $146.5^\circ$ , respectively. The ultraviolet-visible transmittance spectra showed that the transmittance of the superamphiphobic glass was measured to be 85% (Fig. 10c). The transmittance also can be directly observed via a label paper (Fig. 10d). The sufficient hardness and the transmittance make it suitable for many applications, such as windows. Li et al. prepared a translucent

superamphiphobic coating on paper.<sup>139</sup> The optical transmittance values of the coating were more than 45% over the visible range (Fig. 10e). And the visibility of the characters on the paper was almost unchanged (Fig. 10f). Furthermore, the CAs of a series of liquid droplets, ranging from water to organic liquids, were above 150°. Thus, the facile method may lead to commercialization of superamphiphobic paper on a large scale.

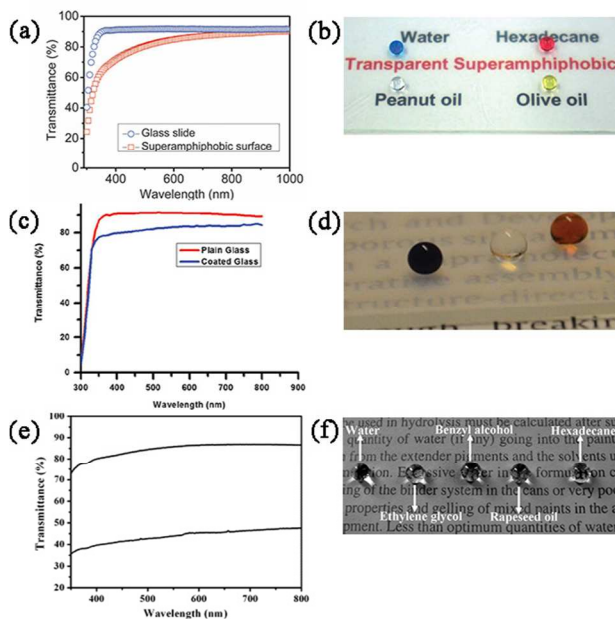


**Fig. 10** Ultraviolet-visible transmittance spectra of (a) 3- $\mu$ m-thick superamphiphobic surface compared with pristine glass, (c) superamphiphobic coated glass surface compared with plain surface and (e) the coated glass substrate compared with the bare glass substrate. Photograph of (b) a drop of dyed water, dyed hexadecane, peanut oil and olive oil deposited on a superamphiphobic glass slide, (d) blue - dyed water, red - dyed hexadecane and colorless ethylene glycol droplets on the superamphiphobic surface and (f) water, ethylene glycol, benzyl alcohol, rapeseed oil and hexadecane droplets on the translucent superamphiphobic paper.<sup>103,138,139</sup> (Copyright from Science 2012)

**4.1.10 Devices.** Water strider can walk on water freely and quickly neither wetting the feet nor cutting through the water.<sup>140</sup> Jiang's group revealed that the legs of water striders are superhydrophobic, on account of hierarchical micro-nano structure and hydrophobic wax material on them.<sup>109,141</sup> Inspired from water strider, Jin et al. designed superhydrophobic and superoleophobic nanocellulose aerogel membranes and proved their applications as cargo carrier on water and oil.<sup>142</sup> The obtained aerogels were made up of unmodified cellulose nanofibers and subsequently modified with fluorosilane. They showed high adhesion, good gas permeability and slightly reduced viscous drag. Moreover, the bio-inspired cargo carriers could support a weight almost 1000 times larger than its own. Lai et al. prepared an anatase TiO<sub>2</sub> particles (ATP) coated Ti substrates and modified with 1H, 1H, 2H, 2H-perfluorodecyltriethoxysilane (PFDS).<sup>143</sup> The surfaces were superoleophobic in air but superoleophilic in water. They applied them as "oil capture hands" to gather oil. In water, the oil droplets were adsorbed to the plates. When taken out from the water, the oil droplets fell off spontaneously. More importantly, there was no oil droplets left on the plates because of their excellent superoleophobicity, which makes it possible for recyclable oil collection.

45

## 4.2 Underwater superoleophobic-superhydrophilic surfaces

At present, the oil pollution caused by marine equipment and offshore oil fields leakage oil has become an urgent problem. And there is an increasing demand for effective, inexpensive, facile methods for cleaning the oily pollution in water. Recently, Jiang and co-workers proposed a new concept of underwater superoleophobicity.<sup>10</sup> They find that marine animals have the ability to move freely no matter how serious the pollution is and keep their surfaces clean. Take lessons from nature, a new idea of utilizing underwater superoleophobic property to solve marine pollution has been raised. Thus, the fabrication and application of underwater superoleophobic surfaces have become a hot topic.

**4.2.1 Self-cleaning.** Similar to superoleophobic surfaces in air, the underwater superoleophobic surfaces also have the self-clean ability for oils. Inspired by the self-clean property of fish scale, Wang et al. prepared underwater superoleophobic conversion films with low adhesion via an in situ alternating-current deposition method.<sup>144</sup> Little wax was stayed on the obtained conversion film when deposition duration was more than 2 h. Moreover, the self-clean surface had a good durability. Hence, the combination of excellent self-cleaning performance and cost-effective fabrication makes it possible to use such films in crude oil pipelines or oil-polluted water. Zhang et al. prepared an underwater superoleophobic mesh by the layer-by-layer (LbL) assembly of sodium silicate and TiO<sub>2</sub> nanoparticles (Fig. 11a).<sup>145</sup> The prepared mesh exhibited self-clean ability after ultraviolet (UV) illumination. In other words, once contaminated by oleic acid, the mesh will lose its hydrophilicity and underwater superoleophobicity, showing hydrophobicity with a WCA of 105° in air. When the contaminated mesh was subject to UV light illumination for 30 minutes, however, the mesh recovered its hydrophilicity as well as underwater superoleophobic property (Fig. 11b). In addition, the self-clean mesh based on UV illumination can be used over and over again with the same property as the original one.

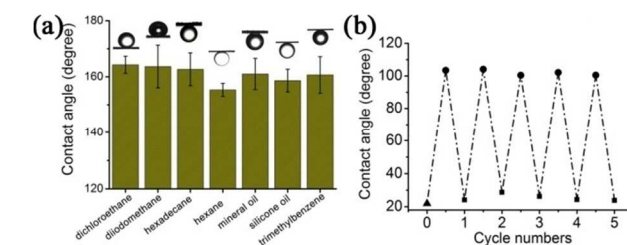


**Fig. 11** (a) Contact angles of a variety of oil droplets on the coated mesh in water, showing superoleophobic property underwater. The insets show the shapes of various oil droplets on the as-prepared mesh surface. (b) The changes of water contact angle on the coated mesh in the five cycles of the oleic acid contamination and UV illumination.<sup>145</sup> (Copyright from Nature 2013)

**4.2.2 Oil-water separation.** Special wettability materials have been used for effectively oil/water separation due to the emission of industrial wastewater and frequently oil spill incident.<sup>27</sup> However, the general superhydrophobic-oleophilic surfaces applied in oil/water separation, especially for membranes, are easily blocking and damaged during the oil permeation process.<sup>146-148</sup> Moreover, on account of the higher density of water, it easily settles and hinders oil penetration. So, it's evitable to find better separation methods for oil-water mixture. Inspired by the skin of shark, many underwater superoleophobic-

superhydrophilic surfaces for water-removing oil/water separation are reported.<sup>149-151</sup> Dong et al. prepared underwater superoleophobic meshes with different pore diameter via coating the hydrophilic graphene oxide (GO) on stainless steel for oil-water separation.<sup>150</sup> They found that both GO coating and suitable pore diameter are crucial to oil-water separation. And the separation efficiency was more than 98% for light oil and 90 % for heavy oil. Moreover, the films can remain underwater superoleophobic after 50 cycles oil/water separation. Zhang et al. designed a bio-inspired chitosan (CS)-coated mesh that can keep stable special wettability in a wide range of pH and hyper-saline solutions due to the formation of stable C-N single bond.<sup>152</sup> The as-prepared mesh can be applied to oil/water separation with relatively high separation efficiency as well. The unique feature is that they can also work well in extreme conditions. In a word, the new method has the advantages of anti-fouling, energy-efficient, cost-efficient, gravity-driven, and recyclable. In addition to common oil-water mixture, even emulsion can be separated by underwater superoleophobic surfaces. Gao et al. prepared ultrathin films for oil-in-water emulsions utilizing single-walled carbon nanotube (SWCNT)/TiO<sub>2</sub> nanocomposite.<sup>153</sup> The films exhibited superhydrophilicity and underwater superoleophobicity after UV-light irradiation, which can separate both a surfactant-free emulsion and a surfactant-stabilized oil-in-water emulsion with very high flux and separation efficiency. In addition, the as-prepared films can maintain their antifouling properties and self-cleaning after multiple cycles on account of the photocatalysis of TiO<sub>2</sub> nanoparticles.

**4.2.3 Device.** Apart from the damage to the environment, oil pollution also hinders the movement of aquatic organisms or devices. The latter will cause huge economy loss. So it is necessary to fabricate devices that can move freely in polluted water. Learning from the water strider, Liu et al. prepared a bio-inspired oil strider by using underwater superoleophobic copper wires as legs (Fig. 12).<sup>154</sup> It is an artificial device that can move freely at the oil-water interface without any oil contamination due to the huge superoleophobic force. The design of the artificial oil strider provides a new idea to fabricate aquatic device with underwater superoleophobicity. The analogous oil strider was prepared by Lai et al., using ATP coated Ti substrates without PFDS modifications.<sup>143</sup> When the artificial oil strider was put on the water, it sank quickly, and finally rest at the oil/water interface. Even severely shake or turn aside, the oil strider still stayed at the oil/water interface. Besides, there were no residual oil on the legs of the above two kinds of oil striders. The success of biomimetic oil-strider will give inspirations to other underwater devices and benefit to our life.

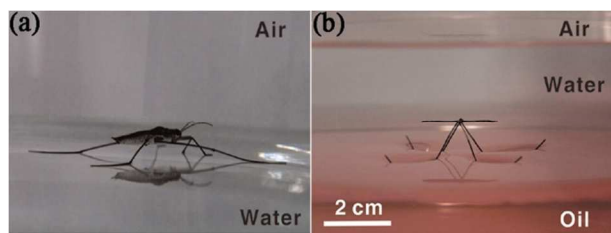


**Fig. 12** The photographs of (a) a water strider at the water/air interface and (b) an artificial oil strider at the oil/water interface. The legs of the oil strider are made up of copper oxide-coated copper wires.<sup>153</sup> (Copyright from ACS 2014)

**4.2.4 Oil droplets manipulation.** Liquid droplets manipulation has drawn extensive attention because of its potential applications in many areas. The manipulation of oil droplets under water is significant because many reactions occur in water environment. Technically, the accurate manipulation for individual oil droplets

can provide less reagent consumption and lower cost for micro-reaction systems. With the aid of outer force or devices, many methods have been explored to manipulate individual liquid droplets, such as optical guide<sup>155</sup> and acoustic field<sup>156</sup>. Different from those, utilizing underwater superoleophobic with low adhesion is facile and low-cost. Su et al. designed a pair of underwater superoleophobic tweezers made of superhydrophilic glass surface on the tips to manipulate oil droplets repeatedly.<sup>157</sup> The study successfully conquered the adhesion problem in oil manipulation. In addition, the coalescence of liquid droplets with different reagents will lead to miniature chemical reaction inside the liquid droplets, which is beneficial to gather valuable products in limited amounts. Besides the artificial oil strider, Lai et al. also built a pair of underwater oil-repellent tweezers, which could capture, lift and transport oils to other superoleophobic surfaces without any oil loss.<sup>143</sup> It is a novel, fluoride-free and low-cost method for on-demand manipulation of oil droplets, which will arouse new ideas for controllable liquid droplets motion and design of simple microreactors.

**4.2.5 Microfluidic channel.** Microfluidic technology has been developed for many years in biology, chemical, and material science. As the microminiaturization of channel, increased viscosity and surface effect can greatly hinder the fluid flow.<sup>158</sup> Due to the anti-oil ability of underwater superoleophobic surfaces, they also can be used for microfluidic channel. Wu et al. created a microfluidic channel by curve-assisted PDMS imprint lithography and demonstrated its anti-oil ability by movies and optical microscopy.<sup>75</sup> Results showed that no oil remained on the hierarchical microstructure region while residual oil on the flat region. The use of superoleophobic surface in microfluidic channel not only greatly extends the applications for anti-oil surfaces but also is a new idea for microfluidic channel.

**4.2.6 Oil transportation.** Transportation of tiny liquid droplets has attracted much attention because of its promising applications in the areas of liquid transportation<sup>25</sup> and lab-on-chip devices<sup>159</sup>. Surface contamination and liquid loss are inevitable in the process of oil transportation.<sup>160</sup> Hence, it is desirable to design surface for no loss oil transportation in a more effective and simple method. Guo et al. prepared an excellent non-wax-stick coating by chemical conversion treatment and evaluated the property through a contrast test.<sup>161</sup> Compared with simple Zn coating, the surface of the as-prepared coating has much less residual of solid wax. Herein, it was indicated that the as-prepared coating had an excellent non-wax-stick ability and can be used for no-loss oil transportation application. Ding et al. designed a polyaniline (PANI) nanowire film with underwater superoleophobicity by electrochemical polymerization.<sup>25</sup> In water, the oil adhesion can be controlled by adjusting electrochemical potential. That is to say, fully reduced states or fully oxidized states make for high adhesion, while intermediate states make for low adhesion. And the contact angles were almost remained constant in this range (Fig. 13a). According to this, no loss oil transportation can be realized. First, an oil droplet was placed on the obtained film (F1) without applying any potential. Then, the same film (F2) applied a voltage of -0.2 was slowly moved to F1. When the oil droplet contacted with both F1 and F2, it would adhere to F2 due to its high adhesion. Likewise, the oil droplet can be transferred back to F1 by applying a voltage of -0.2 (Fig. 13b). Therefore, oil droplets can be transferred one place to another without loss by changing different voltage. These findings will also benefit to explore new applications.

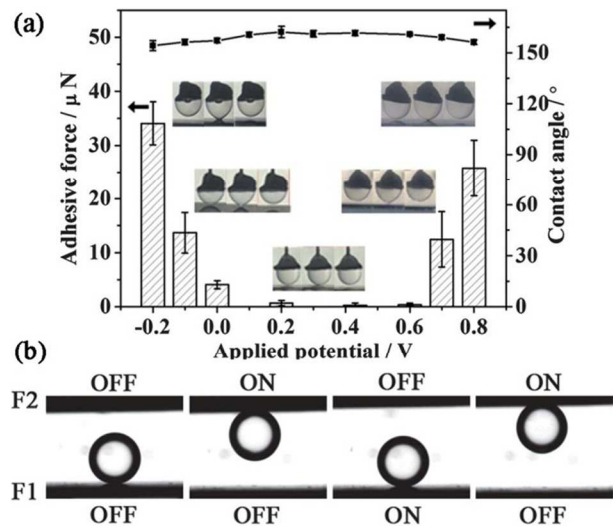


**Fig. 13** (a) Contact angle and adhesive force for an oil droplet in  $0.1 \text{ mol}\cdot\text{L}^{-1} \text{ HClO}_4$  solution when the potential ranged from  $-0.2 \text{ V}$  to  $0.8 \text{ V}$ . (b) The transfer process for an oil droplet from emeraldine salt (ES) state of PANI film to leucoemeraldine form (LEB) state of that applied potential of  $-0.2 \text{ V}$ .<sup>25</sup>

**4.2.7 Bio-adhesion.** Thermally responsive Poly(N-isopropyl acrylamide) (PNIPAAm) has attracted wide attention due to its excellent wetting and platelet adhesion behavior. To be specific, the PNIPAAm surface is hydrophilic and anti-platelets adhesion below the LCST but hydrophobic and platelets adhesive above the LCST.<sup>162</sup> Nanoscale topography was thought to make the surface more hydrophilic and antiadhesive to platelets below the LCST or more hydrophobic and adhesive to platelet above the LCST.<sup>163</sup> However, Chen et al. designed an antiplatelet and thermally responsive PNIPAAm surface with nanoscale topography and proved that this nanoscale structure surface showed anti-platelet adhesion behavior both below and above LCST.<sup>164</sup> Because the platelet adhesion experiment was conducted in phosphate buffered saline, the wetting behavior in liquid solution should be taken into account. The resultant SiNWI-PNIPAAm surface remained underwater superoleophobic property when the temperature was turned from  $20$  to  $37 \text{ }^\circ\text{C}$ , which provided a proof for anti-platelet adhesion at both below and above LCST. It will offer a new strategy for fabricating blood-compatible materials and biomedicine in human body.

### 4.3 Other special wetting surfaces

As research continues, simple superoleophobic surfaces in air or under water can't satisfy the scientists. A large number special superoleophobic surfaces are emerged, which greatly extends the applications of superoleophobic surfaces and makes them perfect.<sup>165</sup> The key factor for special wetting surfaces is choosing suitable modifiers when roughness is enough. Nevertheless, the function of common modifiers is merely reducing the surface tension.

#### 4.3.1 Reversible transitions between underwater superoleophilicity and superoleophobicity

**4.3.1.1 pH induced reversible conversion.** At present, it is reported that carboxyl-terminated polymer makes for realizing

pH induced special wetting surfaces.<sup>166</sup> In fact, it is just a process of protonation and deprotonation. When in acidic and neutral solution, the surface is hydrophobic but oleophilic because of carboxylic acid's protonation. Moreover, according to Wenzel's equation, the oleophilicity increases with the increase of surface roughness.<sup>67</sup> In basic solution, however, the hydrophilicity increases due to deprotonation, and thus generates a water/oil interface, which further increases the surface oleophobicity. When the pH achieves to a certain lever, the surface turns superoleophobic. Inspired by this, many pH-responsive surfaces have been designed. Wang et al. prepared two different smart surfaces on fabrics and copper mesh films by constructing rough structure whereafter modifying with amixture of methyl-terminated thiol ( $\text{HS}(\text{CH}_2)_9\text{CH}_3$ ) and carboxyl-terminated thiol ( $\text{HS}(\text{CH}_2)_{10}\text{COOH}$ ), respectively.<sup>12,167</sup> The as-prepared surface showed superhydrophobic property for acidic and neutral water droplets and superhydrophilic/ superoleophilic property (several minutes later) for basic water droplets in air (Fig. 14a-d). It further leads to underwater superoleophobic property (Fig. 14f). These smart surfaces can be used for a range of applications, take oil/water separation for example. The superoleophobic property also can be reflected in Fig. 14e. For non-basic water, only the oil infiltrated into the as-prepared copper mesh, and the water was retained. Yet when the mesh was first wetted by basic water, the contrary was exactly the case. Hence, water and oil can be selectively separated on the basis of our requirement. Moreover, Cheng et al. also designed a pH-responsive reversible smart surface through similar method and extended the idea to copper mesh and carried out bidirectional oil-water separation.<sup>168</sup> The design of pH induced superoleophilic–superoleophobic surfaces will open up a new door to control surface wettability and further realize more applications.

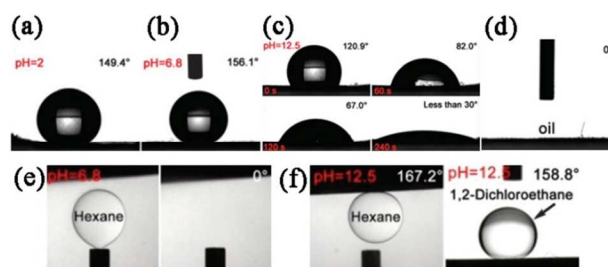


**Fig. 14** Still images of the CAs for an acidic (a), a neutral (b) and a basic (c) water droplet residing on the as-prepared CMF in air, respectively. It is revealed that the surface exhibited superhydrophobicity for acidic and neutral water droplets and superhydrophilicity for basic water droplet (several minutes later). (d) Still image of the oil CA of the CMF in air, showing superoleophilicity of the CMF in air. (e) Still images of the CA for a hexane droplet at neutral aqueous environment ( $\text{pH} = 6.8$ ), showing the superoleophilicity in water. (f) Still images of the CA for hexane and 1,2-dichloroethane droplets at basic aqueous environment ( $\text{pH} = 12.5$ ), respectively. The underwater superoleophobic property was reflected.<sup>12</sup>

**4.3.1.2 Concentration variation induced conversion.** Except for the conversion between underwater superoleophilicity and superoleophobicity induced by pH, concentration also can change surface wettability. Cheng et al. fabricated an underwater superoleophilic/superoleophobic surface by simply changing the

concentration of  $\text{HS}(\text{CH}_2)_{11}\text{OH}$  in the mixture of  $\text{HS}(\text{CH}_2)_9\text{CH}_3$  and  $\text{HS}(\text{CH}_2)_{11}\text{OH}$  on the nanostructured copper substrates.<sup>169</sup> Specifically, when  $-\text{OH}$  concentration increased to a certain value, the surfaces turned to underwater superoleophobic, while the surfaces maintained underwater superoleophilic in low  $-\text{OH}$  concentration. Like other underwater superoleophobic surfaces, it also can be used for oil/water separation selectively. Likewise, the method is suitable for other substrates.

#### 4.3.1.3 Thermo and pH dual-responsive reversible conversion.

Temperature is another factor that can influence the wettability and realize the reversible conversion between underwater superoleophilic property and superoleophobic property. Cao et al. fabricated a thermo and pH dual-responsive material for controllable oil-water separation.<sup>13</sup> Only water can penetrate through the coated mesh when the temperature is less than  $55^\circ\text{C}$  ( $\text{pH} = 7$ ) or  $\text{pH}$  ( $T = 25^\circ\text{C}$ ) less than 13. When PDMAEMA reached  $55^\circ\text{C}$  or  $\text{pH}$  is more than 13, however, oil can pass through the prepared mesh (Fig. 15). The phenomenon was caused by the reduction of the water retention capacity and the swelling volume of the hydrogel. Besides, the protonation degree of the tertiary amine group in PDMAEMA also can influence wettability as the change of  $\text{pH}$ . In this way, oil and water can be selectively separated in situ by adjusting temperature or  $\text{pH}$ .

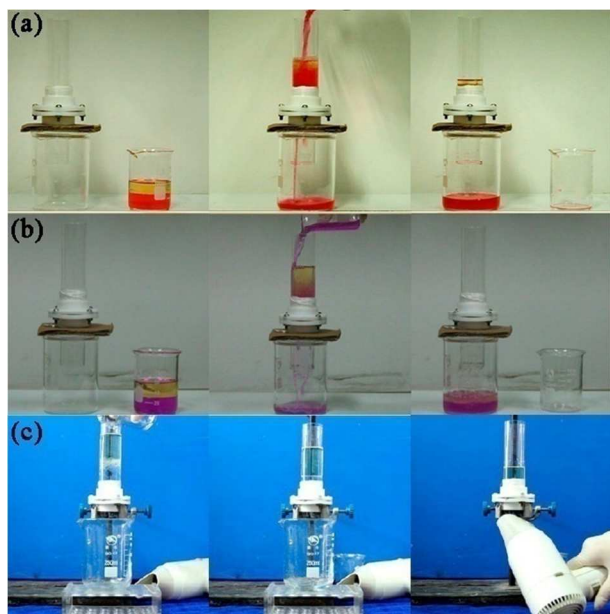


**Fig. 15** Oil/water separation process of the as-prepared dual-responsive surface. (a) When pouring the mixture of gasoline and HCl aqueous solution, water penetrated through rapidly but gasoline was kept on the mesh. (b) The mixture of gasoline and NaOH aqueous solution passed through the mesh altogether. The water was dyed by cresol red, which shows red in the solution with  $\text{pH}$  below 1.8 and purple above 8.0. (c) Only water passed through the mesh at the ambient temperature, and when heated up to its LSCT, gasoline started to permeate the mesh.<sup>13</sup> (Copyright from ACS 2014)

**4.3.2 Superoleophobic-superhydrophilic surface.** Common superoleophobic surfaces in air are also superhydrophobic surfaces as the reason we have mentioned above. There are a few special cases for superoleophobic-superhydrophilic surfaces in air. This is due to the unique interactions between the water/oil and the solid surfaces. Yang et al. have successfully fabricated superoleophobic-superhydrophilic coatings on various substrates

via spray coating with complex polymer (diallyldimethyl ammonium chloride) (PDDA) – sodium perfluorooctanoate (PFO) (the synthesis process is shown in Fig. 16a) modification and finally plasma treatment.<sup>170</sup> The water molecules completely permeated through the treated surfaces while the hexadecane rolled off along the tilted surfaces and then entered into another beaker without being wetted in advance due to water induced molecule rearrangement (Fig. 16b-e). The same process is also suitable for other oils, such as vegetable oil, gasoline, and diesel. Kota et al. designed a superoleophobic-superhydrophilic surfaces both in air and under water through fluorodecyl polyhedral oligomeric silsesquioxane (POSS) and cross-linked poly(ethylene glycol) diacrylate (x-PEGDA).<sup>171</sup> According to the optical microscopy images (Fig. 16f-h), the surface is rough in air while smooth under water, which indicated surface reconfiguration. At the same time, the absence of large scale crystalline domain in situ under water further confirmed this. The obtained surfaces can be used for separation of oil/water mixture and even emulsions with separation efficiency more than 99% and 99.9%, respectively. It's obvious that the special superoleophobic-superhydrophilic surface is more practical than underwater superoleophobic-superhydrophilic surfaces.

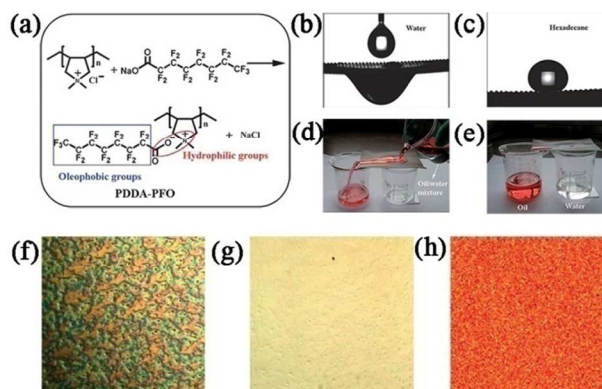


**Fig. 16** (a) The synthesis for PDDA-PFO. (b) Water droplet permeating through the treated mesh. (c) A hexadecane droplet on the mesh with a CA of  $157^\circ$ . (d) and (e) Oil/water separation experiment was performed on the as-prepared mesh. Optical microscopy images of a surface coated with a 20 wt% fluorodecyl POSS + x-PEGDA blend in air (f) and under water (g), respectively. (h) The AFM phase image of a surface coated with a 20 wt% fluorodecyl POSS + x-PEGDA in situ. The phase angle range is from  $0^\circ$  to  $112^\circ$ .<sup>170,171</sup> (Copyright from Nature 2007)

**4.3.3 Superoleophobic property both in air and water.** The roughness with dual-scale structure is required for superoleophobic surfaces both in air and underwater, but the required surface energy materials are opposite. Hence, it's difficult to design surfaces with superoleophobicity for both in air and seawater simultaneously. In some cases, however, oil-repellency both in air and underwater is desirable, such as coatings for marine devices.<sup>104</sup> To this end, Zhang et al. designed a superoleophobic surface both in air and artificial seawater via a polyelectrolyte multilayer (PEM) assembled on an hierarchical aluminum substrate.<sup>11</sup> When immerse in seawater, the perfluorooctanoate (PFO) was replaced by  $\text{Cl}^-$  and  $\text{SO}_4^{2-}$ , making the surface hydrophilic and oleophobic underwater. When remove from seawater, the superoleophobicity of the surface in air recovered by immersing it in a PFO solution. The method can be extended to many other substrates, making it promising to be applied in many areas.

## 5 Conclusions and outlooks

In this review, the recent developments of superoleophobic surfaces have been briefly summarized. In addition, some typical creatures with special wettable surfaces have also been introduced in detail. Much attention is focused on the fabrication and application of various superoleophobic surfaces. Through years of efforts, great progress has been made in the area. But there are still some shortages in industrial production and practical application. First, the fabrication technology is immature. Many fabrications are only limited to laboratory. Second, the mechanical stability of the superoleophobic surface is poor. Even if mass production, the superoleophobic surfaces can't be put into use because of their insufficient mechanical stability. Third, self-healing ability will be enhanced for superoleophobic surfaces because most of the obtained surfaces are easy to lose their superoleophobic property after several cycles of use. Fourth, even if the suitable surfaces are prepared, they still can't be used on a large scale because of their high cost. It's necessary to design proper superoleophobic surfaces with less cost.

To overcome the problems we have mentioned above, more attentions are needed. First and foremost, fundamental research on superoleophobic surfaces is still of great value, especially for structure design. Secondly, the fabrications should be as simple as possible and be easy to repeat. Thirdly, durability and mechanical strength of superoleophobic surfaces in various environments should be taken into account. Last but not least, common, inexpensive, and non-toxic materials should be used for mass production. In short, a bright future of superoleophobic surfaces will be witnessed since more and more scientists spare no effort to design and fabricate such surfaces for their great value.

## Notes and references

<sup>a</sup>Hubei Collaborative Innovation Centre for Advanced Organic Chemical Materials and Ministry of Education Key Laboratory for the Green Preparation and Application of Functional Materials, Hubei University, Wuhan 430062, China.

<sup>b</sup>State Key Laboratory of Solid Lubrication, Lanzhou Institute of Chemical Physics, Chinese Academy of Sciences, Lanzhou 730000, China.

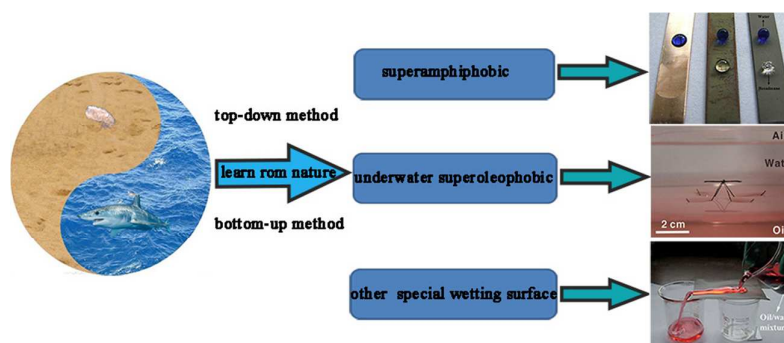
\*Corresponding author. Tel: 0086-931-4968105; Fax: 0086-931-8277088. Email address: zguo@icp.cas.cn (Guo)

- 1 (a) G. Wang, Z. Guo and W. Liu, *J. Bionic Eng.*, 2014, **11**, 325. (b) S. Yu, Z. G. Guo, and W. M. Liu, *Chem. Commun.* 2014, DOI: 10.1039/C4CC06868H.
- 2 J. Xu and Z. Guo, *J. Colloid Interface Sci.*, 2013, **406**, 1.
- 3 (a) Y. Zhang, Y. Chen, L. Shi, J. Li and Z. Guo, *J. Mater. Chem.*, 2012, **22**, 799. (b) W. X. Liang, G. Y. Wang, B. Wang, Y. B. Zhang, Z. G. Guo, *Acta. Chim. Sinica*. 2013, **71**, 639.
- 4 B. Wang, W. Liang, Z. Guo and W. Liu, *Chem. Soc. Rev.*, 2014, DOI: 10.1039/c4cs00220b.
- 5 L. Feng, S. H. Li, Y. S. Li, H. J. Li, L. J. Zhang, J. Zhai, Y. L. Song, B. Q. Liu, L. Jiang and D. B. Zhu, *Adv. Mater.*, 2002, **14**, 1857.
- 6 A. Tuteja, W. Choi, M. L. Ma, J. M. Mabry, S. A. Mazzella, G. C. Rutledge, G. H. McKinley and R. E. Cohen, *Science*, 2007, **318**, 1618.
- 7 H. J. Li, X. B. Wang, Y. L. Song, Y. Q. Liu, Q. S. Li, L. Jiang and D. B. Zhu, *Angew. Chem., Int. Ed.*, 2001, **40**, 1743.
- 8 A. K. Kota, W. Choi and A. Tuteja, *MRS Bull.*, 2013, **38**, 383.
- 9 T. P. N. Nguyen, R. Boukherroub, V. Thomy and Y. Coffinier, *J. Colloid Interface Sci.*, 2014, **416**, 280.
- 10 M. Liu, S. Wang, Z. Wei, Y. Song and L. Jiang, *Adv. Mater.*, 2009, **21**, 665.
- 11 G. Zhang, X. Zhang, Y. Huang and Z. Su, *ACS Appl. Mater. Interfaces*, 2013, **5**, 6400.
- 12 B. Wang and Z. Guo, *Chem. Commun. (Camb)*, 2013, **49**, 9416.
- 13 Y. Cao, N. Liu, C. Fu, K. Li, L. Tao, L. Feng and Y. Wei, *ACS Appl. Mater. Interfaces*, 2014, **6**, 2026.
- 14 H. Ollivier, *Ann. Chim. Phys.*, 1907, **10**, 229.
- 15 T. Onda, S. Shibuichi, N. Satoh and K. Tsujii, *Langmuir*, 1996, **12**, 2125.
- 16 C. Neinhuis and W. Barthlott, *Ann. Bot.*, 1997, **79**, 667.
- 17 W. Barthlott and C. Neinhuis, *Planta*, 1997, **202**, 1.
- 18 L. Jiang, Y. Zhao and J. Zhai, *Angew. Chem., Int. Ed.*, 2004, **43**, 4338.
- 19 G. R. J. Artus, J. Zimmermann, F. A. Reifler, S. A. Brewer and S. Seeger, *Appl. Surf. Sci.*, 2012, **258**, 3835.
- 20 T. Darmanin and F. Guittard, *J. Colloid Interface Sci.*, 2013, **408**, 101.
- 21 L. P. Xu, J. Peng, Y. Liu, Y. Wen, X. Zhang, L. Jiang and S. Wang, *ACS Nano*, 2013, **7**, 5077.
- 22 J. Yang, H. J. Song, B. B. Chen, H. Tang and C. S. Li, *RSC Adv.*, 2014, **4**, 14227.
- 23 A. Siriviriyannun and T. Imae, *Chem. Eng. J.*, 2014, **246**, 254.
- 24 H. Zhao and K. Y. Law, *Langmuir*, 2012, **28**, 11821.
- 25 C. M. Ding, Y. Zhu, M. J. Liu, L. Feng, M. X. Wan and L. Jiang, *Soft Matter*, 2012, **8**, 9064.
- 26 Z. Z. Zhang, X. T. Zhu, J. Yang, X. H. Xu, X. H. Men and X. Y. Zhou, *Appl. Phys. A*, 2012, **108**, 601.
- 27 Q. S. Liu, A. A. Patel and L. Y. Liu, *ACS Appl. Mater. Interfaces*, 2014, **6**, 8996.
- 28 Z. G. Guo and W. M. Liu, *Plant Sci.*, 2007, **172**, 1103.
- 29 Z. Guo, W. Liu and B. L. Su, *J. Colloid Interface Sci.*, 2011, **353**, 335.
- 30 Y. M. Zheng, X. F. Gao and L. Jiang, *Soft Matter*, 2007, **3**, 178.
- 31 K. S. Liu and L. Jiang, *Nano Today*, 2011, **6**, 155.
- 32 S. G. Lee, H. S. Lim, D. Y. Lee, D. Kwak and K. Cho, *Adv. Funct. Mater.*, 2013, **23**, 547.
- 33 H. Zhu, Z. G. Guo and W. M. Liu, *Chem. Commun.*, 2014, **50**, 3900.
- 34 A. R. Parker and C. R. Lawrence, *Nature*, 2001, **414**, 33.
- 35 S. J. Hong, C. C. Chang, T. H. Chou, Y. J. Sheng and H. K. Tsao, *J. Phys. Chem. C*, 2012, **116**, 26487.
- 36 L. Feng, Y. A. Zhang, J. M. Xi, Y. Zhu, N. Wang, F. Xia and L. Jiang, *Langmuir*, 2008, **24**, 4114.
- 37 X. F. Gao, X. Yan, X. Yao, L. Xu, K. Zhang, J. H. Zhang, B. Yang and L. Jiang, *Adv. Mater.*, 2007, **19**, 2213.
- 38 R. Helbig, J. Nicklerl, C. Neinhuis and C. Werner, *Plos One*, 2011, **6**, 10.1371/journal.pone.0025105.
- 39 R. Hensel, R. Helbig, S. Aland, H. G. Braun, A. Voigt, C. Neinhuis and C. Werner, *Langmuir*, 2013, **29**, 1100.
- 40 A. B. D. Cassie and S. Baxter, *Trans. Faraday Soc.*, 1944, **40**, 0546.
- 41 B. Bhushan, *Beilstein J. Nanotechnol.*, 2011, **2**, 66.
- 42 G. D. Bixler and B. Bhushan, *Soft Matter*, 2012, **8**, 11271.
- 43 G. D. Bixler and B. Bhushan, *J. Colloid Interface Sci.*, 2013, **393**, 384.
- 44 G. D. Bixler and B. Bhushan, *Nanoscale*, 2013, **5**, 7685.
- 45 S. Nishimoto and B. Bhushan, *RSC Adv.*, 2013, **3**, 671.
- 46 Q. Cheng, M. Li, Y. Zheng, B. Su, S. Wang and L. Jiang, *Soft Matter*, 2011, **7**, 5948.
- 47 J. M. Osborn and E. L. Schneider, *Ann. Mo. Bot. Gard.*, 1988, **75**, 778.
- 48 X. L. Liu, J. Zhou, Z. X. Xue, J. Gao, J. X. Meng, S. T. Wang and L. Jiang, *Adv. Mater.*, 2012, **24**, 3401.
- 49 J. F. Wang, Q. F. Cheng and Z. Y. Tang, *Chem. Soc. Rev.*, 2012, **41**, 1111.
- 50 J. F. Wang, L. Lin, Q. F. Cheng and L. Jiang, *Angew. Chem., Int. Ed.*, 2012, **51**, 4676.
- 51 Q. F. Cheng, L. Jiang and Z. Y. Tang, *Acc. Chem. Res.*, 2014, **47**, 1256.
- 52 J. F. Wang, Q. F. Cheng, L. Lin and L. Jiang, *ACS Nano*, 2014, **8**, 2739.
- 53 Q. F. Cheng, M. X. Wu, M. Z. Li, L. Jiang and Z. Y. Tang, *Angew. Chem., Int. Ed.*, 2013, **52**, 3750.
- 54 K. Liu, J. Du, J. Wu and L. Jiang, *Nanoscale*, 2012, **4**, 768.
- 55 J. Ma, Y. Sun, K. Gleichauf, J. Lou and Q. Li, *Langmuir*, 2011, **27**, 10035.
- 56 A. K. Epstein, B. Pokroy, A. Seminara and J. Aizenberg, *Proc. Natl. Acad. Sci. U. S. A.*, 2011, **108**, 995.

- 57 H. C. Yang, J. K. Pi, K. J. Liao, H. Huang, Q. Y. Wu, X. J. Huang and Z. K. Xu, *ACS Appl. Mater. Interfaces.*, 2014, **6**, 12566.
- 58 Y. Cai, L. Lin, Z. X. Xue, M. J. Liu, S. T. Wang and L. Jiang, *Adv. Funct. Mater.*, 2014, **24**, 809.
- 59 W. Ma, H. Xu and A. Takahara, *Adv. Mater. Interf.*, 2014, **1**, 10.1002/admi.201300092.
- 60 W. Cui, M. Z. Li, J. Y. Liu, B. Wang, C. Zhang, L. Jiang and Q. F. Cheng, *ACS Nano*, 2014, **8**, 9511.
- 61 Q. F. Cheng, M. Z. Li, L. Jiang and Z. Y. Tang, *Adv. Mater.*, 2012, **24**, 1838.
- 62 T. Z. Wu and Y. Suzuki, *Sensor Actuat. B*, 2011, **156**, 401.
- 63 R. T. R. Kumar, K. B. Mogensen and P. Boggild, *J. Phys. Chem. C*, 2010, **114**, 2936.
- 64 S. E. Lee, H. J. Kim, S. H. Lee and D. G. Choi, *Langmuir*, 2013, **29**, 8070.
- 65 S. M. Kang, S. M. Kim, H. N. Kim, M. K. Kwak, D. H. Tahk and K. Y. Suh, *Soft Matter*, 2012, **8**, 8563.
- 66 T. Darmanin and F. Guittard, *Soft Matter*, 2013, **9**, 5982.
- 67 R. N. Wenzel, *Ind. Eng. Chem.*, 1936, **28**, 988.
- 68 H. Bellanger, T. Darmanin, E. T. de Givenchy and F. Guittard, *Chem. Rev.*, 2014, **114**, 2694.
- 69 S. Ji, P. A. Ramadhianti, T. B. Nguyen, W. D. Kim and H. Lim, *Microelectron. Eng.*, 2013, **111**, 404.
- 70 X. T. Zhu, Z. Z. Zhang, X. H. Xu, X. H. Men, J. Yang, X. Y. Zhou and Q. J. Xue, *J. Colloid Interface Sci.*, 2012, **367**, 443.
- 71 J. F. Ou, W. H. Hu, S. Liu, M. S. Xue, F. J. Wang and W. Li, *ACS Appl. Mater. Interfaces*, 2013, **5**, 10035.
- 72 J. L. Song, S. Huang, K. Hu, Y. Lu, X. Liu and W. J. Xu, *J. Mater. Chem. A*, 2013, **1**, 14783.
- 73 K. Ellinas, S. P. Pujari, D. A. Dragatogiannis, C. A. Charitidis, A. Tserepi, H. Zuilhof and E. Gogolides, *ACS Appl. Mater. Interfaces*, 2014, **6**, 6510.
- 74 M. Im, H. Im, J. H. Lee, J. B. Yoon and Y. K. Choi, *Soft Matter*, 2010, **6**, 1401.
- 75 D. Wu, S. Z. Wu, Q. D. Chen, S. Zhao, H. Zhang, J. Jiao, J. A. Piersol, J. N. Wang, H. B. Sun and L. Jiang, *Lab Chip*, 2011, **11**, 3873.
- 76 K. Ellinas, A. Tserepi and E. Gogolides, *Langmuir*, 2011, **27**, 3960.
- 77 H. B. Jo, J. Choi, K. J. Byeon, H. J. Choi and H. Lee, *Microelectron. Eng.*, 2014, **116**, 51.
- 78 H. J. Choi, S. Choo, J. H. Shin, K. I. Kim and H. Lee, *J. Phys. Chem. C*, 2013, **117**, 24354.
- 79 S. Anandan, T. N. Rao, M. Sathish, D. Rangappa, I. Honma and M. Miyauchi, *ACS Appl. Mater. Interfaces*, 2013, **5**, 207.
- 80 C. J. Chang, C. F. Wang, J. K. Chen, C. C. Hsieh and P. A. Chen, *Appl. Surf. Sci.*, 2013, **286**, 280.
- 81 M. Paulose, H. E. Prakasam, O. K. Varghese, L. Peng, K. C. Popat, G. K. Mor, T. A. Desai and C. A. Grimes, *J. Phys. Chem. C*, 2007, **111**, 14992.
- 82 S. Barthwal, Y. S. Kim and S. H. Lim, *J. Colloid Interface Sci.*, 2013, **400**, 123.
- 83 S. Nishimoto, Y. Sawai, Y. Kameshima and M. Miyake, *Chem. Lett.*, 2014, **43**, 518.
- 84 S. Barthwal, Y. S. Kim and S. H. Lim, *Langmuir*, 2013, **29**, 11966.
- 85 J. L. Yong, F. Chen, Q. Yang, D. S. Zhang, U. Farooq, G. Q. Du and X. Hou, *J. Mater. Chem. A*, 2014, **2**, 8790.
- 86 T. Buhrike, A. Kibellus and A. Lampen, *Toxicol. Lett.*, 2013, **218**, 97.
- 87 A. Drame, T. Darmanin, S. Y. Dieng, E. T. de Givenchy and F. Guittard, *RSC Adv.*, 2014, **4**, 10935.
- 88 T. Darmanin, J. Tarrade, E. Celia and F. Guittard, *J. Phys. Chem. C*, 2014, **118**, 2052.
- 89 H. Bellanger, T. Darmanin, E. T. de Givenchy and F. Guittard, *J. Mater. Chem. A*, 2013, **1**, 2896.
- 90 J. Tarrade, T. Darmanin, E. T. de Givenchy and F. Guittard, *RSC Adv.*, 2013, **3**, 10848.
- 91 Y. Lu, J. L. Song, X. Liu, W. J. Xu, Y. J. Xing and Z. F. Wei, *ACS Sustainable Chem. Eng.*, 2013, **1**, 102.
- 92 H. Wang and Z. Guo, *Appl. Phys. Lett.*, 2014, **104**, 183703.
- 93 J. Zeng and Z. Guo, *Colloids Surf., A*, 2014, **444**, 283.
- 94 G. Hayase, K. Kanamori, G. Hasegawa, A. Maeno, H. Kaji and K. Nakanishi, *Angew. Chem., Int. Ed.*, 2013, **52**, 10788.
- 95 Y. Li, X. T. Zhu, X. Y. Zhou, B. Ge, S. W. Chen and W. S. Wu, *Appl. Phys. A*, 2014, **115**, 76.
- 96 A. K. Kota, Y. Li, J. M. Mabry and A. Tuteja, *Adv. Mater.*, 2012, **24**, 5838.
- 97 V. A. Ganesh, S. S. Dinachali, A. S. Nair and S. Ramakrishna, *ACS Appl. Mater. Interfaces*, 2013, **5**, 1527.
- 98 F. Ejaz Ahmed, B. S. Lalia, N. Hilal and R. Hashaikheh, *Desalination*, 2014, **344**, 48.
- 99 M. A. Gondal, M. S. Sadullah, M. A. Dastageer, G. H. McKinley, D. Panchanathan and K. K. Varanasi, *ACS Appl. Mater. Interfaces*, 2014, **6**, 13422.
- 100 O. U. Nimittrakoolchai and S. Supothina, *J. Nanosci. Nanotechnol.*, 2012, **12**, 4962.
- 101 S. Pechook, N. Kornblum and B. Pokroy, *Adv. Funct. Mater.*, 2013, **23**, 4572.
- 102 P. Aminayi and N. Abidi, *Appl. Surf. Sci.*, 2013, **287**, 223.
- 103 X. Deng, L. Mammen, H. J. Butt and D. Vollmer, *Science*, 2012, **335**, 67.
- 104 L. P. Xu, J. Zhao, B. Su, X. L. Liu, J. T. Peng, Y. B. A. Liu, H. L. Liu, G. Yang, L. Jiang, Y. Q. Wen, X. J. Zhang and S. T. Wang, *Adv. Mater.*, 2013, **25**, 606.
- 105 S. S. Latthe, C. Terashima, K. Nakata, M. Sakai and A. Fujishima, *J. Mater. Chem. A*, 2014, **2**, 5548.
- 106 G. Zhou, J. H. He, L. J. Gao, T. T. Ren and T. Li, *RSC Adv.*, 2013, **3**, 21789.
- 107 J. J. Yuan and R. H. Jin, *Langmuir*, 2011, **27**, 9588.
- 108 A. Das, T. M. Schutzius, I. S. Bayer and C. M. Megaridis, *Carbon*, 2012, **50**, 1346.
- 109 T. Sun, L. Feng, X. Gao and L. Jiang, *Acc. Chem. Res.*, 2005, **38**, 644.
- 110 G. D. Bixler, A. Theiss, B. Bhushan and S. C. Lee, *J. Colloid Interface Sci.*, 2014, **419**, 114.
- 111 Y. Y. Liu, X. Q. Chen and J. H. Xin, *Bioinspir. Biomim.*, 2008, **3**, 1.
- 112 K. Naderi and T. Babadagli, *Energ. Fuel.*, 2013, **27**, 6501.
- 113 W. W. Zhang, T. T. Wang and S. C. Zhang, *Appl. Mech. Mater.*, 2014, **472**, 338.
- 114 A. J. DeMello, *Nature*, 2006, **442**, 394.
- 115 X. Yao, J. Gao, Y. L. Song and L. Jiang, *Adv. Funct. Mater.*, 2011, **21**, 4270.
- 116 Y. C. Jung and B. Bhushan, *Langmuir*, 2009, **25**, 14165.
- 117 M. Jin, J. Wang, X. Yao, M. Liao, Y. Zhao and L. Jiang, *Adv. Mater.*, 2011, **23**, 2861.
- 118 G. Y. Wang, H. R. Wang and Z. G. Guo, *Chem. Commun.*, 2013, **49**, 7310.
- 119 S. W. Chang, C. M. Chen and J. L. He, *Adv. Mater. Res.*, 2012, **509**, 132.
- 120 B. Bhushan and P. Muthiah, *Microsyst. Technol.*, 2013, **19**, 1261.
- 121 P. Muthiah, B. Bhushan, K. Yun and H. Kondo, *J. Colloid Interface Sci.*, 2013, **409**, 227.
- 122 R. Kasada and P. Dou, *J. Nucl. Mater.*, 2013, **440**, 647.
- 123 H. X. Liu, Q. Xu, Y. H. Jiang, C. Q. Wang and X. W. Zhang, *Surf. Coat. Technol.*, 2013, **228**, S538.
- 124 Y. H. Yu, Y. Y. Lin, C. H. Lin, C. C. Chan and Y. C. Huang, *Polym. Chem.*, 2014, **5**, 535.
- 125 Z. Q. Yuan, J. Y. Xiao, C. Q. Wang, J. C. Zeng, S. L. Xing and J. Liu, *J. Coat. Technol. Res.*, 2011, **8**, 773.
- 126 N. V. Motlagh, F. C. Birjandi, J. Sargolzaei and N. Shahtahmassebi, *Appl. Surf. Sci.*, 2013, **283**, 636.
- 127 B. Ge, Z. Zhang, X. Men, X. Zhu and X. Zhou, *Appl. Surf. Sci.*, 2014, **293**, 271.
- 128 H. Q. Liu, S. Szunerits, W. G. Xu and R. Boukherroub, *ACS Appl. Mater. Interfaces*, 2009, **1**, 1150.
- 129 S. Pan, A. K. Kota, J. M. Mabry and A. Tuteja, *J. Am. Chem. Soc.*, 2013, **135**, 578.
- 130 K. Y. Law and H. Zhao, *Nip 25: Digital Fabrication 2009, Technical Program and Proceedings*, 2009, 53.
- 131 H. Zhao and K. Y. Law, *ACS Appl. Mater. Interfaces*, 2012, **4**, 4288.
- 132 S. H. Au, P. Kumar and A. R. Wheeler, *Langmuir*, 2011, **27**, 8586.
- 133 G. Perry, V. Thomy, M. R. Das, Y. Coffinier and R. Boukherroub, *Lab Chip*, 2012, **12**, 1601.
- 134 S. L. Freire and B. Tanner, *Langmuir*, 2013, **29**, 9024.

- 135 P. Mazumder, Y. Jiang, D. Baker, A. Carrilero, D. Tulli, D. Infante, A. T. Hunt and V. Pruneri, *Nano Lett.*, 2014, **14**, 4677.
- 136 H. M. Shang, Y. Wang, S. J. Limmer, T. P. Chou, K. Takahashi and G. Z. Cao, *Thin Solid Films*, 2005, **472**, 37.
- 5 137 X. Yao, Y. Song and L. Jiang, *Adv. Mater.*, 2011, **23**, 719.
- 138 V. A. Ganesh, S. S. Dinachali, H. K. Raut, T. M. Walsh, A. S. Nair and S. Ramakrishna, *RSC Adv.*, 2013, **3**, 3819.
- 139 J. Li, L. Yan, Q. L. Ouyang, F. Zha, Z. J. Jing, X. Li and Z. Q. Lei, *Chem. Eng. J.*, 2014, **246**, 238.
- 10 140 M. A. Samaha, H. V. Tafreshi and M. Gad-el-Hak, *C.R. Mec.*, 2012, **340**, 18.
- 141 X. Q. Feng, X. F. Gao, Z. N. Wu, L. Jiang and Q. S. Zheng, *Langmuir*, 2007, **23**, 4892.
- 142 H. Jin, M. Kettunen, A. Laiho, H. Pynnonen, J. Paltakari, A. Marmur, O. Ikkala and R. H. A. Ras, *Langmuir*, 2011, **27**, 1930.
- 15 143 Y. K. Lai, Y. X. Tang, J. Y. Huang, F. Pan, Z. Chen, K. Q. Zhang, H. Fuchs and L. F. Chi, *Sci. Rep.*, 2013, **3**, 3009.
- 144 Z. Wang, L. Zhu, W. Li and H. Liu, *ACS Appl. Mater. Interfaces*, 2013, **5**, 10904.
- 20 145 L. Zhang, Y. Zhong, D. Cha and P. Wang, *Sci. Rep.*, 2013, **3**, 2326.
- 146 J. Li, L. Shi, Y. Chen, Y. B. Zhang, Z. G. Guo, B. L. Su and W. M. Liu, *J. Mater. Chem.*, 2012, **22**, 9774.
- 147 X. M. Tang, Y. Si, J. L. Ge, B. Ding, L. F. Liu, G. Zheng, W. J. Luo and J. Y. Yu, *Nanoscale*, 2013, **5**, 11657.
- 25 148 F. Zhao, L. L. Liu, F. J. Ma and L. Liu, *RSC Adv.*, 2014, **4**, 7132-7135.
- 149 Y. Z. Zhu, F. Zhang, D. Wang, X. F. Pei, W. B. Zhang and J. Jin, *J. Mater. Chem. A*, 2013, **1**, 5758-5765.
- 150 Y. Dong, J. Li, L. Shi, X. Wang, Z. Guo and W. Liu, *Chem. Commun. (Camb)*, 2014, **50**, 5586-5589.
- 30 151 W. B. Zhang, Y. Z. Zhu, X. Liu, D. Wang, J. Y. Li, L. Jiang and J. Jin, *Angew. Chem., Int. Ed.*, 2014, **53**, 856-860.
- 152 S. Zhang, F. Lu, L. Tao, N. Liu, C. Gao, L. Feng and Y. Wei, *ACS Appl. Mater. Interfaces*, 2013, **5**, 11971-11976.
- 35 153 S. J. Gao, Z. Shi, W. B. Zhang, F. Zhang and J. Lin, *ACS Nano*, 2014, **8**, 6344-6352.
- 154 X. L. Liu, J. Gao, Z. X. Xue, L. Chen, L. Lin, L. Jiang and S. T. Wang, *ACS Nano*, 2012, **6**, 5614-5620.
- 155 F. M. Weinert, C. B. Mast and D. Braun, *Phys. Chem. Chem. Phys.*, 2011, **13**, 9918-9928.
- 40 156 G. Yu, X. L. Chen and J. Xu, *Proceedings of the Asme International Mechanical Engineering Congress and Exposition, 2011, Vol 6, Pts a and B*, 2012, 1153-1158.
- 157 B. Su, S. Wang, Y. Song and L. Jiang, *Soft Matter*, 2011, **7**, 5144.
- 45 158 J. West, A. Michels, S. Kittel, P. Jacob and J. Franzke, *Lab Chip*, 2007, **7**, 981.
- 159 L. Ionov, N. Houbenov, A. Sidorenko, M. Stamm and S. Minko, *Adv. Funct. Mater.*, 2006, **16**, 1153.
- 160 T. Verho, C. Bower, P. Andrew, S. Franssila, O. Ikkala and R. H. A. Ras, *Adv. Mater.*, 2011, **23**, 673.
- 50 161 Y. Z. Guo, W. P. Li, L. Q. Zhu and H. C. Liu, *Mater. Lett.*, 2012, **72**, 125.
- 162 K. Uchida, K. Sakai, E. Ito, O. H. Kwon, A. Kikuchi, M. Yamato and T. Okano, *Biomaterials*, 2000, **21**, 923.
- 55 163 T. Sun, G. Wang, L. Feng, B. Liu, Y. Ma, L. Jiang and D. Zhu, *Angew. Chem.*, 2004, **43**, 357.
- 164 L. Chen, M. J. Liu, H. Bai, P. P. Chen, F. Xia, D. Han and L. Jiang, *J. Am. Chem. Soc.*, 2009, **131**, 10467.
- 165 Q. F. Cheng, M. Z. Li, F. Yang, M. J. Liu, L. Li, S. T. Wang and L. Jiang, *Soft Matter*, 2012, **8**, 6740.
- 60 166 N. Fauchoux, R. Schweiss, K. Lutzow, C. Werner and T. Groth, *Biomaterials*, 2004, **25**, 2721.
- 167 B. Wang, Z. G. Guo and W. M. Liu, *RSC Adv.*, 2014, **4**, 14684.
- 168 Z. J. Cheng, H. Lai, Y. Du, K. W. Fu, R. Hou, C. Li, N. Q. Zhang and K. N. Sun, *ACS Appl. Mater. Interfaces*, 2014, **6**, 636.
- 65 169 Z. J. Cheng, H. Lai, Y. Du, K. W. Fu, R. Hou, N. Q. Zhang and K. N. Sun, *ACS Appl. Mater. Interfaces*, 2013, **5**, 11363.
- 170 J. Yang, Z. Zhang, X. Xu, X. Zhu, X. Men and X. Zhou, *J. Mater. Chem.*, 2012, **22**, 2834.
- 70 171 A. K. Kota, G. Kwon, W. Choi, J. M. Mabry and A. Tuteja, *Nat. Commun.*, 2012, **3**, 1025.





Recent progress of biomimetic superoleophobic surfaces in fabrications and applications are mainly reviewed, and current and further challenges for biomimetic superoleophobic surfaces are also proposed.